Modeling and Simulation of the Controllable Network Transformers

Oyelami Kazeem Opeyemi

Submitted to the
Institute of Graduate Studies and Research
in partial fulfillment of the requirements for the Degree of

Master of Science
in
Electrical and Electronics Engineering

Eastern Mediterranean University
January 2012
Gazimağusa, North Cyprus

Approval of the Institute of Graduate Studies and Research

Prof. Dr. Elvan Yılmaz
Director

I certify that this thesis satisfies the requirements as a thesis for the degree of Master of Science in Electrical and Electronic Engineering.

Assoc. Prof. Dr. Aykut Hocanın
Chair, Department of Electrical Electronic and Engineering

We certify that we have read this thesis and that in our opinion it is fully adequate in scope and quality as a thesis for the degree of Master of Science in Electrical and Electronic Engineering.

Prof. Dr. Osman Kükrer
Supervisor

Examining Committee

1. Prof. Dr. Osman Kükrer
2. Prof. Dr. Hasan Kömürcügil
3. Prof. Dr. Runyi Yu

ABSTRACT

The work presented in this thesis looked into the working principle of the Controllable Network Transformer in controlling the flow of power through tie lines. It has always been difficult to control the power flowing through the tie lines that connect two areas. This causes a lot of stress on the power grid and makes it weak as time goes on. There had been a number of ways of controlling this flow of power and this has proven to achieve a limited amount of control. The previous method had made use of devices such as the Load tap Changing Transformers and Phase Shifting Transformers.

The controllable transformer is introduced as a simple device that was realized by augmenting a fraction of a centre-tapped or a Linear Tap Changing transformer (LTC) with a small bidirectional low-rated AC-AC converter.

The dual virtual quadrature sources (DVQS) scheme was also developed and used as against the conventional Pulse Width Modulation. This DVQS makes use of the Even Harmonic Modulation techniques (EHM) by injecting a series of voltage sources between the two buses to control both the magnitude and direction of the flow of power in the model.

This thesis discussed the basics, modeling and theoretical analyses of the CNT extensively. The derived equations were then compared with results obtained from simulations using MATLAB simulink. The Simulations of the CNT Model was

discussed extensively in Chapter Three. During the simulations, each elements of the model were tested to see their contributions to the model.

It was also observed that there are huge amount of third harmonics in the circuit. These are unwanted, hence a third-harmonic trap was designed to reduce or remove the unwanted third harmonics in the circuit.

The effect of the DC component K_0 of the reference voltage, the second harmonic amplitude K_2 and the phase angle φ on the Power output were also considered.
The bidirectional control property of the CNT on the power flow was also considered.

Finally, we also developed the Variable Structural System control of the CNT. This enabled us to analyze the full working principle of the CNT and the effect of the duty cycle *d* on the overall performance of the CNT model.

The advantages and the shortcomings of the CNT as compared to the other power flow controller were also analyzed and discussed under the discussion section in Chapter 3.

Keywords: Controllable Network Transformer (CNT), Dual Virtual Quadrature Scheme (DVQS), Even harmonic modulation (EHM), Smart grid, Power flow control.

ÖZ

Bu tez, denetlenebilir şebeke trafosunun bir bağlantı hattı üzerinden geçen gücü kontrol etmesinin çalışma ilkeleri üzerinde durmaktadır. İki enerji tesis bölgesi arasındaki güç akışını denetlemek her zaman sorun yaratmıştır. Bu sorun şebeke üzerinde baskı yaratmakta ve onun kararlı çalışmasını zayıf hale getirmektedir. Bölgeler arası güç akışını denetlemek için bazı yöntemler uygulanmış, fakat kontrol edilebilen güç miktarı sınırlı olmuştur. Bu yöntemler yük altında kademe değiştiren trafolar (LTC) ve faz kaydıran trafolar kullanmaktadır.

Denetlenebilir şebeke trafosu bu sorunları çözmek için önerilmiş basit yapıda bir cihaz olup, bir LTC ve düşük güçlü ve iki yönlü bir AA-AA çeviriciden oluşmaktadır. İkili sanal kaynak düzeneği (DVQS) ise geleneksel DGM (Darbe Genişliği Modülasyonu)'na alternatif olarak geliştirilip kullanılmaktadır. DVQS çift harmonik modülasyon yöntemini kullanıp iki taşıyıcı arasındaki güç akışının miktar ve yönünü kontrol etmek için bu ikisinin arasında bir dizi gerilim kaynağı oluşturmaktadır.

Bu tez CNT'nin temel ilkeleri, modellenmesi ve kuramsal çözümlemelerini geniş bir biçimde tartışmaktadır. Elde edilen denklemler, MATLAB Simulink ile elde edilen sonuçlarla karşılaştırılmıştır.

CNT modelinin benzetimleri 3'ncü bölümde geniş bir biçimde tartışılmıştır. Benzetim çalışmaları sırasında her eleman modele katkısını görmek için sınanmıştır.

Ayrıca devrede büyük miktarlarda üçüncü harmonik olduğu gözlenmiştir. Bunlar istenmediğinden, devreden giderilebilmeleri için üçüncü harmonik tuzağı (süzgeçi) tasarlanmıştır.

Referans işaretinin DA bileşeninin, ikinci harmonik tepe değeri K_2'nin ve faz açısı φ'nin güç akışı üzerindeki etkileri de incelenmiştir. Ayrıca, CNT'nin iki yönlü güç akışını denetleme özelliği üzerinde de durulmuştur.

Son olarak, CNT'nin yapısal değişken dizge modeli geliştirildi. Bu model bize CNT'nin çalışma ilkelerini daha iyi çözümleme, ve anahtar elemanlarının görev oranının (*d*) CNT'nin davranışına olan etkisini inceleme imkanı verdi.
Diğer güç akış denetleyicilere göre CNT'nin avantaj ve sorunları da tartışılmıştır.

Anahtar sözcükler: Denetlenebilir Şebeke Trafosu, İkili sanal kaynak, Çift harmonic modülasyonu, Akıllı şebeke, Güç akışı kontrolu.

My Dad, Mum and Siblings.

ACKNOWLEDGMENTS

I would like to offer my sincerest appreciation to my supervisor Prof. Dr. Osman Kükrer who has supported me throughout my research work & write-up of this thesis, with patience all along. This thesis would not have been possible without his support and guidance. I couldn't have imagined having a better supervisor and a mentor for my postgraduate studies.

Also, my sincere thanks definitely go to Assoc. Prof. Dr. Aykut Hocanın, the Chair of our department, for his great assistance in my early enrolment process to the department. I will also like to thank Assoc. Prof. Dr. Hasan Demirel for his many supports and fatherly advices.

I convey my special thanks to my friends and colleagues specially Halidu Sule, Nazzal, Edmund, Quadri and Pouya.

Words would fail to express my greatest appreciation towards my parents & my siblings, for their inseparable support, gentle love and prayers.

TABLE OF CONTENTS

LIST OF TABLES

LIST OF FIGURES

LIST of SYMBOLS & ABBREVIATIONS

AC	Alternate Current
BTB	Back To Back HVDC link
CNT	Controllable Network Transformer
DVQS	Dual Virtual Quadrature Sources
EHM	Even Harmonic Modulation
FACTS	Flexible AC transmission system
LTC	Load Tap Changer
OPF	Optimal Power Flows
PST	Phase Shifting Transformers
PWM	Pulse Width Modulation
STATCOM	Static Synchronous Compensator
TACC	Thin AC Converter
UPFC	Unified Power Flow Controller
VFT	Variable Frequency Transformer
VSS	Variable Structure System
d	Duty cycle
C_f	Forward capacitor
C_{trap}	Trap capacitor
K_0	DC Component

K_2	Second harmonic amplitude
L	Line Inductance
n	Tap ratio
Pu	Per unit
δ	Phase difference
ϕ	Phase angle
Ω	Ohms

Chapter 1

INTRODUCTION

1.1 Power Flow

Smart Grids are comprised of devices to control the flow of electrons. Power flow control devices increase the potential and capacity of the whole or overall system, without the need of building new transmission lines.

Power flow devices are the integral part of smart grids and they use different strategies in modulating the flow of power, thereby increasing the efficiency of the power grid.

In recent times, power grids had been built extensively in a more radial structure. These transmission and distribution lines had been constructed in such a way to directly connect the generating facility to the load centers.

This has been shown to be highly undependable. A fault on the line could cause the entire network or system to breakdown. Thus electric transmission in a more mesh network has been advocated for; this allows a fault to be easily isolated.

1.2 Power Flow Control

Transmission lines are often built in a radial structure; they use tie-lines to connect two areas together. Power flowing through the tie-lines connecting two areas is often very difficult to control. This is as a result of increased load demand, high level of renewable energy and low investment in the transmission infrastructure. This problem has increased the need for a smart controllable grid [1].

Presently, utilities have little or no control over power flowing through the tie-lines [2]. Often in the case of contingencies, tie-lines gets overloaded and trip off and may eventually see power flow in the opposite direction [2]

Thus electric transmission in mesh networks has been called for and it is very important to control the power flow in such a network.

Here are some means by which power flow is controlled.

1. The use of Optimal Power Flow Techniques
2. Phase-Shifting Transformer
3. Use of FACTs (Flexible AC transmission system)
4. Variable Frequency Transformer (VFT)

5 Controllable Network Transformer (CNT)

1.2.1 Optimal Power Flows

This is the use of powerful algorithms to set the operating points of various generators, shunt VAR compensation and Load Tap Changing (LTC) tap settings [1].

The main objective of this optimal power flow control is to acquire the complete voltage angle and the magnitude information for each bus in power systems, which is required to accommodate specific load and produce voltage and real power conditions.

Once the required data are obtained (by the use of algorithms), the real and reactive power flow on the buses as well as the generator reactive power outputs are determined.

The optimal power flow (OPF) problems are solved using algorithms by determining the known and unknown variables involved in a power systems. These variables depend on the kind of the bus in use (load bus and generator bus).

Because the OPF is a very large, non-linear mathematical programming problem, it has taken decades to develop efficient algorithms for its solution [3]. The different techniques of the optimal power flow control are as follows.

1. Lambda iteration method [11]
2. Gradient method [10]
3. Newton's method [12]
4. Linear Programming method [13]
5. Interior point method [14]

The OPF performs all systems control while maintaining the system security. This control include generator outputs, transformer tap changing ,transformer phase shifts, while maintaining and ensuring that no power component limits are violated [3].

Maintenance of the system security requires keeping each device in the power system within its desired operating range at steady state. This includes maximum and minimum output for generators, maximum MVA flows on transmission lines and transformers as well as keeping system bus voltage with specific ranges [3].

1.2.1.1 Shunt VAR compensation and LTC

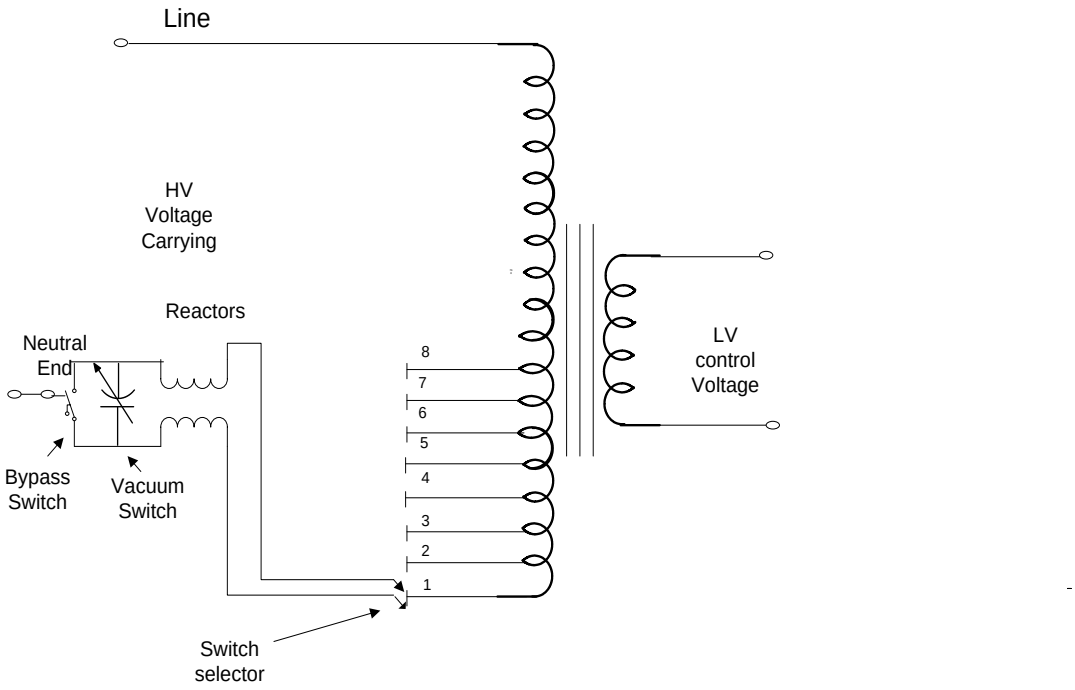

Figure 1.1 Load Tap Changer Transformers [19].

Shunt VAR compensation and Load Tap-Changing (LTC) are both used to regulate the bus voltages.

Shunt VAR compensation reduces the generated harmonics. The LTC however provides some control on the power flowing through the line by controlling the

magnitude of the bus voltage [2].The typical LTC transformer connection is seen in Figure 1.1.

The control range of both shunt VAR compensation and LTC are very small and hence it will be very expensive to use for a long ranged transmission line. This is because the bus voltage needs to be regulated for a long ranged transmission line and in a small band [2]. Also the changes in voltage usually cause significant amount of loop current in the system. This causes power to add up and removed in the form of heat, thereby decreases the efficiency of the transformer.

1.2.2 Phase Shifting Transformers.

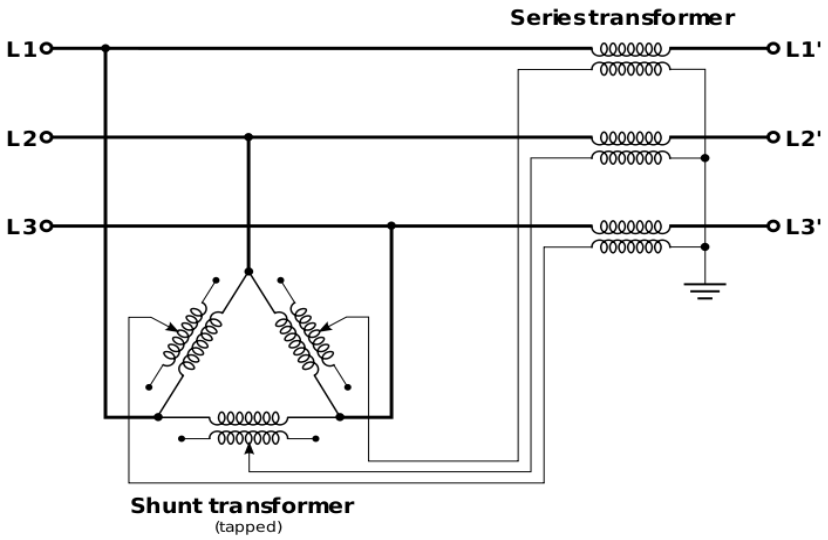

Figure 1.2 Phase Shifting Transformer [20].

Phase shifting transformers as shown in Figure (1.2), are used to control the phase angle between the source and the load. They create a shift between the primary side and the secondary side voltage.

They are used to control the flow of power over transmission lines. They control both the magnitude and phase angle by varying the phase shift.

Theoretically, phase shifting transformer is considered as a sinusoidal AC voltage source with controllable amplitude and phase [4].

The control achieved is slow and the connections between the different inter-phases lead to complex faults mode [2].

1.2.3 Flexible AC Transmission Systems (FACTS)

Flexible AC transmission systems, (FACTS) were developed based on power electronics to improve the performance of long distance AC transmission. It was later extended to a device that can control power flow.

FACTS uses power electronics as the basis to provide solution to operational challenges in AC transmission over a large scale. It allows for a minimal infrastructure investment, environmental impacts and implementation time for the construction of a new transmission line [15].

FACTS works either by controlling the voltage or by modifying the impedance of the transmission line to control the power flow.

Although FACTS is the modern basis of controlling the power flow in transmission lines, one of its major short-comings is that the amount of power to be transmitted over the line is limited. This is a result of heat losses (from the conductors) in case of short line or voltage drops and thermal loss in long range lines.

1.2.3.1 Unified Power Flow Controller (UPFC)

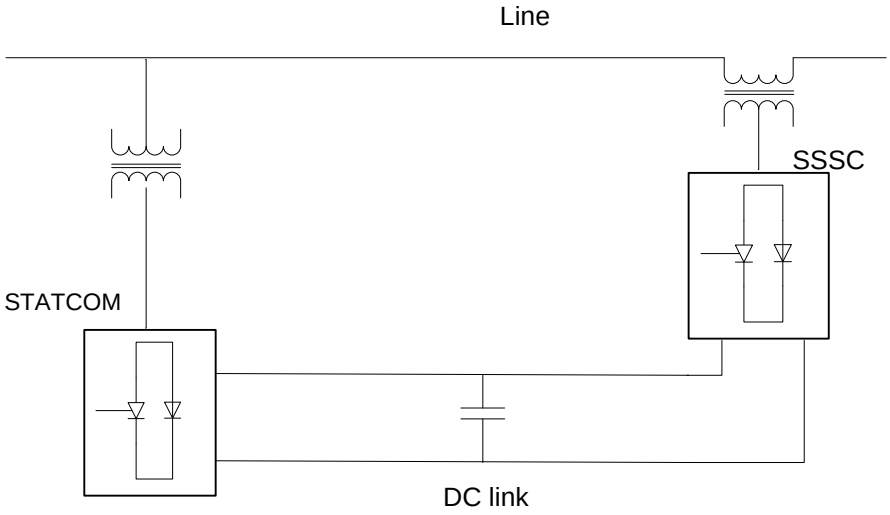

Figure 1.3: The UPFC consisting of the STATCOM and SSSC controllers [15].

The UPFC combines the STATCOM and SSSC controllers and thus provides smooth simultaneous control of all basic power systems parameters (transmission, impedance, phase angle). It has the function of reactive shunt compensation, series compensation and phase shifting to achieve the control of power flow.

UPFC controls both the line current and the voltage by injecting voltage compensation in series and current in the shunt as seen in Figure (1.3).

The shunt compensation generates or absorbs reactive power, thus providing independent shunt reactive compensation.

The series compensation injects voltage with controllable magnitude and phase angle, in series with the line through a voltage source [5].

1.2.3.2 Back To Back (BTB) HVDC link

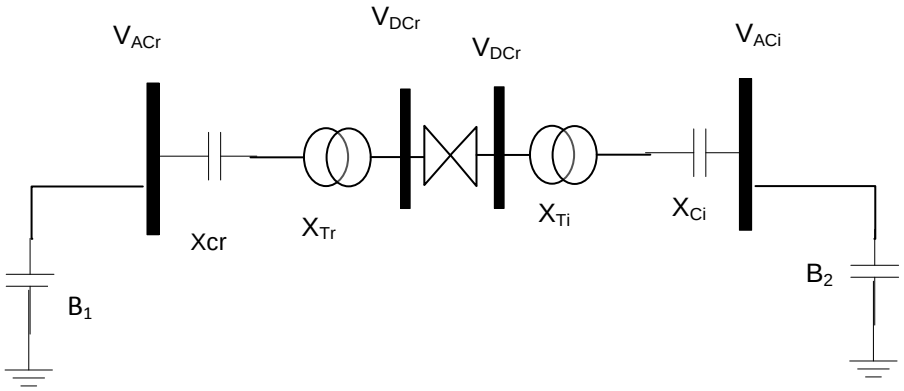

Figure 1.4: A simple diagram showing the BTB HVDC link connections [16].

It is used to connect two areas and it uses two bidirectional converters (voltage source) that exchanges power from a common DC link [16] as seen in Figure (1.4). It provides a wide range of control and connects two asynchronous systems. It controls both the active and reactive power continuously across the entire operating range.

1.2.4 Voltage Frequency Transformer (VFT)

VFT allows power flow between two asynchronous networks. It is very similar to back to back HVDC as it is also bidirectional in nature.

The VFT is essentially a continuous variable phase shifter that has the potential of working at an adjustable phase angle. It is a rotary transformer with a three phase winding on both rotor and stator [6]. One power grid is connected to the rotor side of the VFT and another connected to the stator side of the VFT [6].

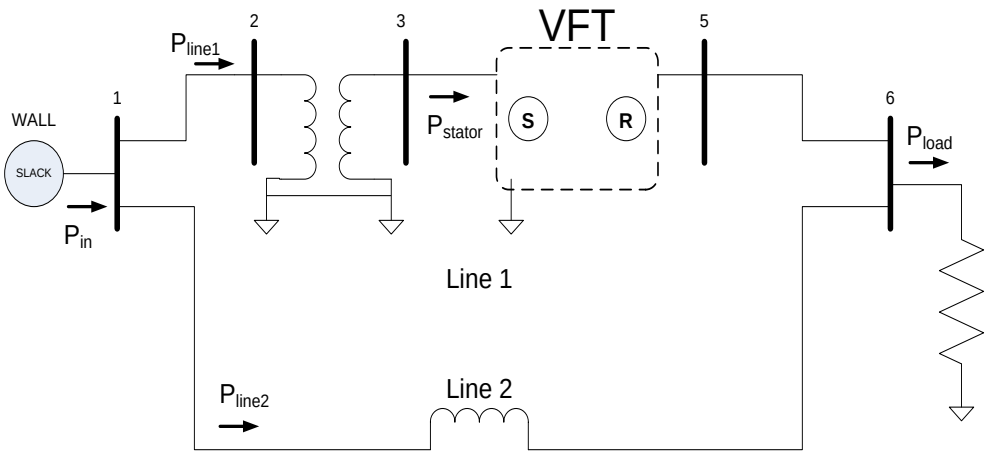

Figure 1.5: Diagram showing a VFT simple model [18].

The flow of power in a system is proportional to the angle of the rotational transformer and as with other AC power circuit. The impedance of the rotary transformer, and AC grid determine the magnitude of the phase shift required for a given power transfer [6].

Unlike BTB and UPFC that uses power electronic switches and are thus capable of producing sub cycle transient responses, VFTs are electromechanical devices which are slower, with response time on the order of 1-2s [2].

The devices discussed above (UPFC,BTB,VFTs) have the tendency of smooth controlling the flow of power, but their usage at transmission level or even the sub-transmission level are expensive and very complex to build[2].

1.2.5 Introduction to the Controllable Network Transformer

The CNT is realized by augmenting LTC with small fractionally rated bidirectional direct AC-AC converters [7]. It is used to control both the magnitude and as well as the phase angle of the bus voltage by the use of a dual virtual quadrature sources scheme (DVQS) [2]. This enables the CNT to achieve a more accurate power flow control in a meshed network system.

This thesis looked into the theoretical analysis and the operations of the CNT in a mesh network. It also looked into the detailed simulations of CNT with regards to controlling the power flow in a mesh network. Implementations at the transmission and sub transmission level voltages were also put into consideration.

The results from the experimental simulations of the CNT using MATLAB simulink were also discussed.

The implementation, control and usage are then compared with other power flow controllers like VTF, BTB and the UPFC.

Chapter 2

CONTROLLABLE NETWORK TRANSFORMER

2.1 Controllable Network Transformer

A Controllable Network Transformer (CNT) comprises a centre-tapped or a Linear Tap Changing transformer (LTC) and a small bidirectional low-rated AC-AC converter [2].

This AC-AC converter is comprised of two AC switches, a small filter capacitor and an inductor [2]. The converter is fractionally rated with respect to the ratings of the centre-tapped transformer used. This allows the CNT to have a wide control of the whole system.

The Controllable Network Transformer (CNT) provides simultaneous control of the bus voltages and the phase angles.

The CNT basics as well as its principle of working are discussed in the next section.

2.2 Controllable Network Transformer basics

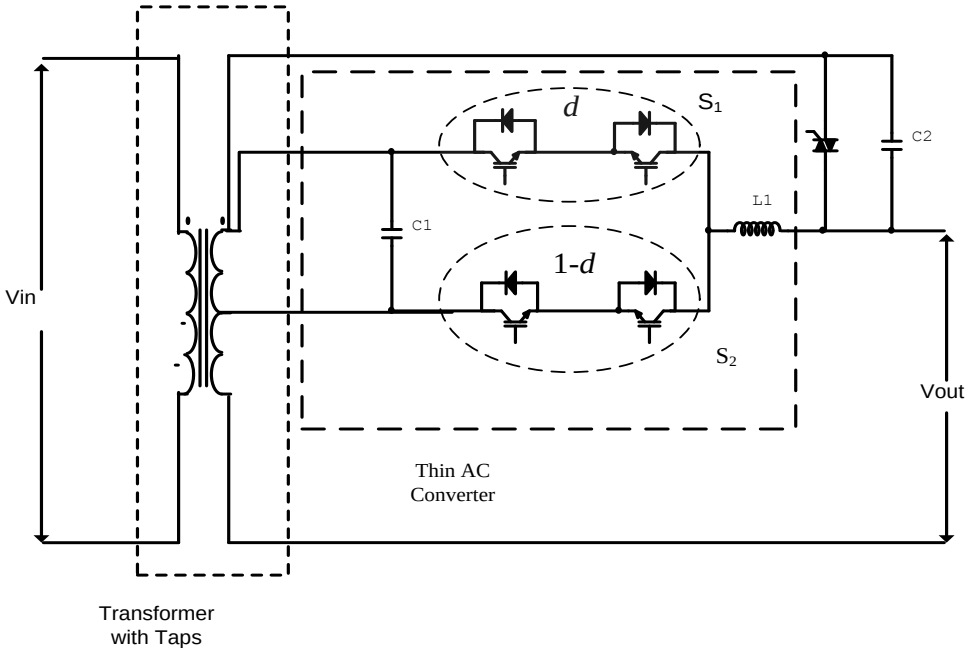

Figure 2.1: Controllable Network Transformer [2].

In this chapter, the full description of the CNT is discussed in accordance with the paper in [2].The analysis and modeling of the CNT were also put into consideration. We also carried out some experimental simulations in Chapter 3 of this thesis, using MATLAB Simulink, to verify the claims and authenticity of the procedures performed in the paper.

In Figure 2.1, the CNT consists of a centre-tapped transformer and two AC-AC switches. The switches labeled S_1 and S_2 are operated at fixed duty cycles of *d* and 1-*d* respectively. Let the CNT have a terminal tap ratio *n*. If the switch S_1 is ON, the turn's ratio of the transformer will be 1: 1+ *n*. Also, if S_2 is ON, the turn ratios will be 1:1- *n*. By applying a fixed duty ratio *d*, it is possible to achieve an output voltage magnitude between $\frac{1}{1+n}$ to $\frac{1}{1-n}$ pu. [2].

The CNT is proposed to be able to control both the voltages and the phase angles. Using conventional PWM, it is hard to control the phase angle of the resulting output voltage.

This is due to the fact that there are no energy-storage devices in the system, which usually allow for switching over or zero crossing of the input voltage.

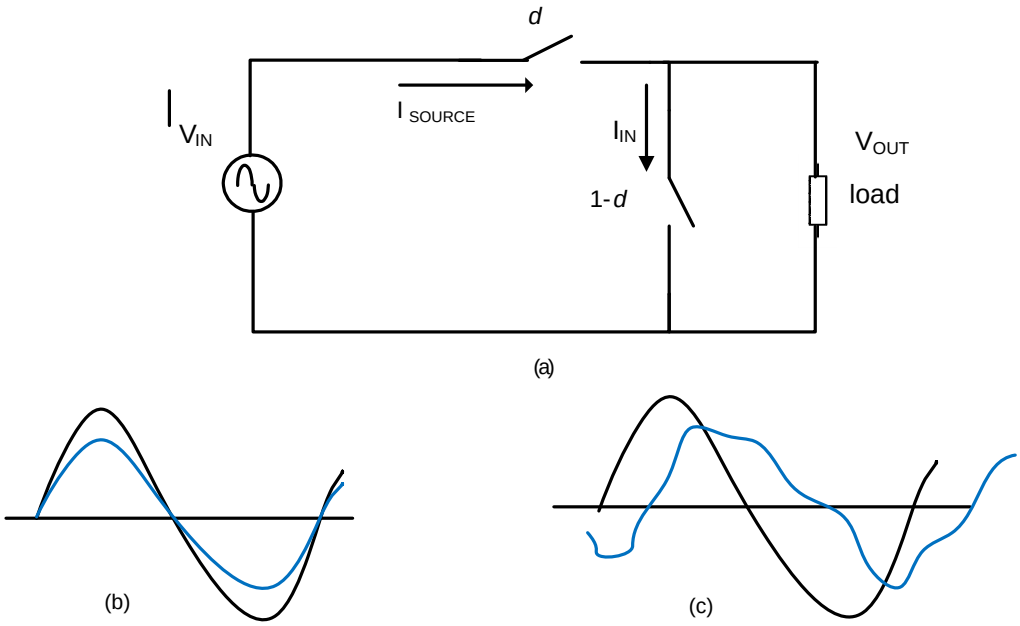

Figure 2.2: AC chopper (a) Circuit topology (b) Achievable output voltage (c) Unachievable output voltage using conventional PWM [2].

It can be seen from the simple AC chopper circuit shown in Figure 2.2, using the conventional PWM, the CNT is able to control the magnitude of the output voltage but has no control over the phase angle. Therefore the output voltage in this case is of the same phase as that of the input voltage but of lesser magnitude [2].

This leads to the concept of creating dual virtual quadrature sources (DVQS), that allows the synthesis of output voltages with controllable phases or harmonic level without requiring the use of stored energy or an additional source and switches [7].

2.3 Dual Virtual Quadrature Scheme

To be able to control the phase angle of the output voltage, dual virtual quadrature scheme (DVQS) is applied [2].

When the DVQS technique is applied, the output voltage is made up of three components. The first component is the output voltage (V_{do}) that is in phase with the input voltage. In addition, two other sources are invoked in quadrature to the input voltage.

One of these sources is at the fundamental frequency (V_{qo}) and the other is at the third harmonic frequency (V_3). The sum of all these three components at all instances of time lies within the envelope of the input voltage [2]. The output obtained at the fundamental frequency is a result of the sum of the components V_{d0} and $V_{q0.}$

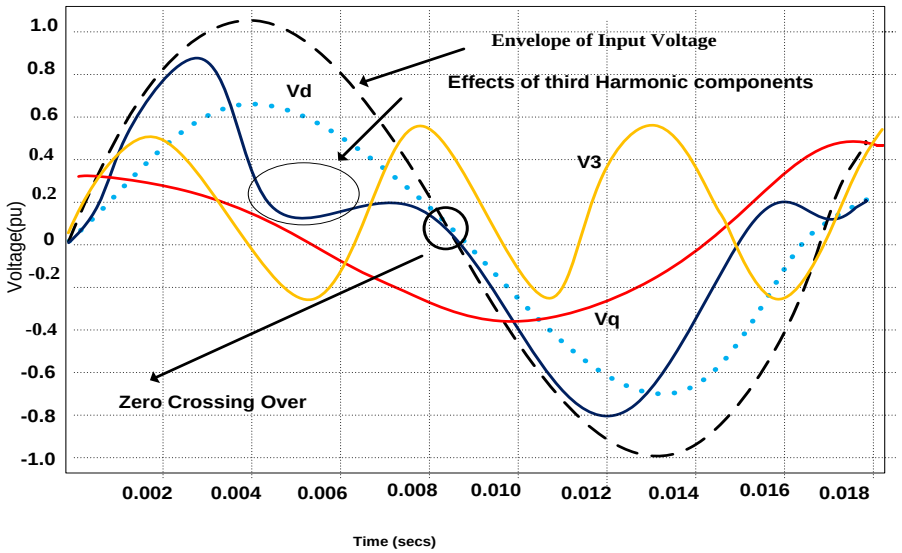

Figure 2.3: Various components of the output voltage obtained using DVQS strategy[2]

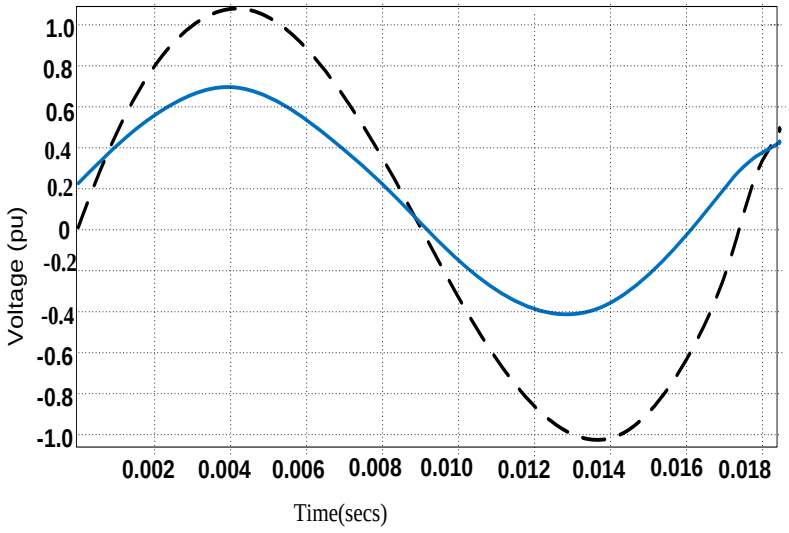

Figure 2.4: Input and phase shifted output voltage [2].

To implement the DVQS, the even harmonic modulation (EHM) technique is used. This allows a CNT that ingest a series of voltage sources between two buses, to control the magnitude and direction of the power flowing in the line connecting them [2].

The even harmonic modulation technique (EHM) allows the use of a simple AC chopper with a sinusoidal AC, and the generation of an output voltage with a desired amplitude, phase angle and or harmonic content by trading off between the fundamental frequency and a harmonic quadrature source [8]. The detailed analysis of a CNT using the DVQS, and the implementation of the even harmonic modulation scheme (EHM) are discussed in the next section.The experimental simulations are also analysed in Charpter 3 of this thesis.

2.4 Analysis and Model Derivation of a CNT

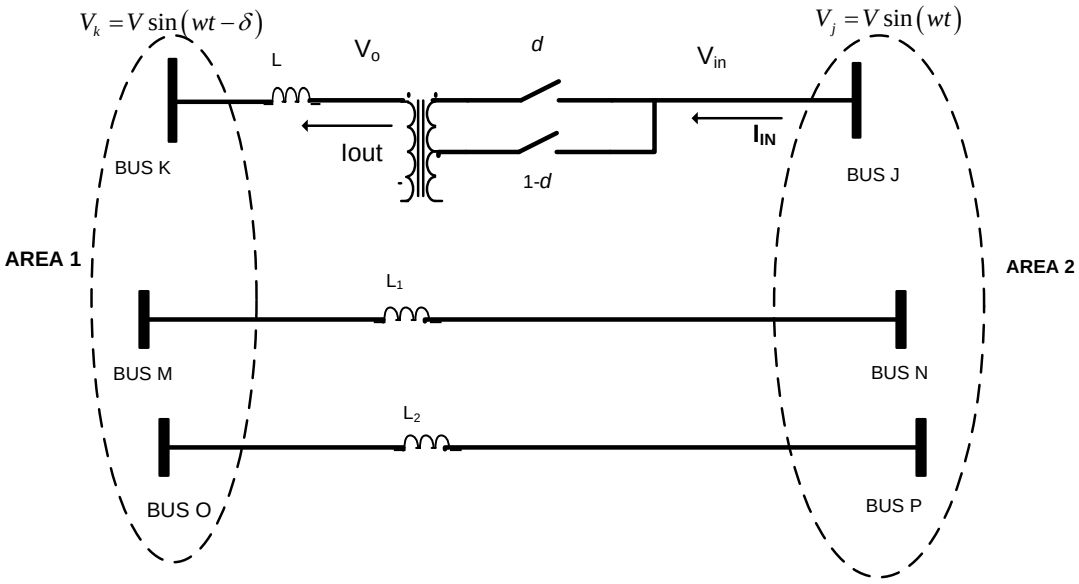

Figure 2.5: Controllable network transformer on a tie line connecting control areas 1 and 2

The CNT model on a transmission line is shown in Figure 2.5. It is placed on the tie line between two control areas 1 and 2. These two areas may be connected to one or more tie-lines.

The CNT is assumed to be connected between bus J and K, and their voltages are assumed to be separated by a phase difference of δ.

The sum of the inductances of the transmission line and that of the transformer reflected to area1 is L. The losses in the transmission line and the CNT are assumed to be neglected. The DVQS is implemented using the even harmonic scheme (EHM) [8]. The scheme is carried out using sine-triangle PWM, by using a control reference voltage consisting of a dc component K_0, a second harmonic of amplitude K_2 and a phase angle φ .

The duty cycle of switch S_1 is given by

$$d = K_0 + K_2 \sin(2\omega t + \phi) \tag{1.1}$$

At Bus J

$$V_J = V_{in} = V_1 sin\omega t \tag{1.2}$$

At Bus *K*

$$V_K = V_O = V_2 \sin(\omega t - \delta) \tag{1.3}$$

Voltage V_O (that is the output voltage at the CNT) can be expressed in terms of the input voltage V_{in}, duty cycle d, and tap ratio n.

$$V_O = [\ \frac{d}{1+n} + \frac{1-d}{1-n}\ ] V_{in} \tag{1.4}$$

Simplifying putting equation (1.1) into equation (1.4)

$$V_O = [\ \frac{d(1-n) + (1-d)(1+n)}{1+n}\ ]\ V_{in} \tag{1.5}$$

$$V_O = [\ \frac{d(1-n) + (1+n-d-dn)}{1-n^2}\ ]\ V_{in} \tag{1.6}$$

$$V_O = [\frac{1+n-2dn}{1-n^2}]\ V_{in} \tag{1.7}$$

Substituting for $d = K_o + K_2 \sin(2\omega t + \phi)$ in (equation 1.7)

$$V_O = [\frac{1+n-2n[K_o + K_2 \sin(2\omega t + \phi)}{1-n^2}]V_{in} \tag{1.8}$$

$$V_O = [\frac{1+n-2K_o n+2nK_2 \sin(2\omega t + \phi)}{1-n^2}]\ V_1 \sin \omega t \tag{1.9}$$

$$V_O = \frac{(1+n-2K_o n)V_1 \sin \omega t + (2nK_2 \sin(2\omega t + \phi))V_1 \sin \omega t}{1-n^2} \tag{1.10}$$

$$V_O = \frac{(1+n-2K_o n)V_1 \sin \omega t}{1-n^2} + \frac{(2nK_2 \sin(2\omega t + \phi))V_1 sin\omega t}{1-n^2} \tag{1.11}$$

Let $\quad A = \frac{1+n-2K_0 n}{1-n^2}$ (1.12)

$$B = \frac{nK_2}{1-n^2} \tag{1.13}$$

Thus we have

$$V_O = AV_1 sin\omega t + 2BV_1 \sin(2\omega t + \phi)\sin \omega t \tag{1.14}$$

Using the trigonometric identity

$$sinAsinB = \frac{1}{2}\left(\cos\left(A-B\right)-\cos\left(A+B\right)\right)$$

in equation (1.15), we get

$$V_0 = -AV_1\sin\omega t - 2BV_1\frac{1}{2}(\cos(\omega t+\phi)-\cos(3\omega t+\phi)) \quad (1.15)$$

$$V_O = V_1(A\sin\omega t - B\cos(\omega t+\phi)) + BV_1\cos(3\omega t+\phi) \quad (1.16)$$

Expressing the output voltage in phasors notations, V_O becomes

$$V_O^{(1)} = -jV_1A - V_1B(\cos\phi + j\sin\phi) \quad \text{and} \quad V_o^{(3)} = BV_{(1)}\langle\phi \quad (1.17)$$

It can be seen that the simplification of equation (1.4) shows that V_O consists of a fundamental component and a third harmonic component.

The constant K_0 and K_2 are not fully independent of each other. This is illustrated from the constraint equation.

$$K_2 \le \min\{K_0, 1-K_0\} \quad (1.18)$$

This constraint is required to prevent *overmodulation*.

Overmodulation occurs when the peak control voltages exceed the peak of the triangular waveform as regards to pulse width modulation (PWM). It is not a normal operating condition for a multilevel inverter, but in many applications, there are situations where demanded output are usually greater for pulse-dropping to occur.

To avoid over modulation, the summation of the magnitude of the reference voltage, K_0 and that of the second harmonic magnitude, K_2 must be less than 1.

The secondary current, I_o, can be expressed in terms of phasors as follows.

$$I_o^{(1)} = \frac{V_o^1 - V_k}{j\omega L} \quad \text{and} \quad I_o^{(3)} = \frac{V_0^3}{j(3\omega)L} \tag{1.19}$$

Corresponding to the fundamental component, V_o^1 and the third harmonic component of V_0, (V_0^3).

Combining equations (1.19) and substituting equation (1.3) and (1.17), the current I_o in time function becomes

$$I_o(t) = -\frac{AV_1}{\omega L}\cos(\omega t) - \frac{BV_1}{\omega L}\sin(\omega t + \phi) + \frac{V_2}{\omega L}\cos(\omega t - \delta) + \frac{V_1}{3\omega L} B\sin(3\omega t + \phi) \tag{1.20}$$

Also by the principle of conservation of energy, the input and output currents are related by

$$I_{in} = \left[\frac{d}{1+n} + \frac{1-d}{1-n}\right] I_o \tag{1.21}$$

Substituting equation (1.21) in (1.22)

$$I_{in} = \frac{V_1}{\omega L}(-A^2 + \frac{2}{3}B^2)\cos(\omega t - \delta) + \frac{V_2}{\omega L}(A\cos(\omega t - \delta) - B\sin(\omega t + \phi + \delta) + \frac{BV_1}{\omega L}(2A\sin(3\omega t + \phi) - B\cos(3\omega t + 2\phi) - \frac{BV_2}{\omega L}\sin(3\omega t + \phi - \delta) + \frac{B^2V_1}{3\omega L}\cos(5\omega t + 2\phi) \tag{1.22}$$

From equation (1.22), the input current is seen to consist of the fundamental, third and fifth harmonic components. Since the CNT consists majorly of passive devices, the input and the output power must be of the same value. This is verified by comparing equations (1.1) and (1.19), and equations (1.2) and (1.22).

Power flowing through the transmission line without the CNT is given by

$$P_{line} = \frac{V_1 V_2}{\omega L} sin\delta \tag{1.23}$$

When the CNT is connected across the line, the real power through the line will be

$$P_{LINE_{CNT}} = \frac{V_1 V_2}{\omega L}\left(Asin\delta - \mathrm{B}\cos\left(\delta + \phi\right)\right) \tag{1.24}$$

While the sending-end reactive power will be

$$Q_{SEND} = \frac{V_1^2}{\omega L}\left(A^2 - \frac{2}{3} B^2 \right) - \frac{A V_1 V_2}{\omega L} cos\delta + \frac{\mathrm{B} V_1 V_2}{\omega L} \sin\delta \tag{1.25}$$

Equations (1.24) and (1.25) provide useful understanding into the working principles of the controllable network transformer. The fundamental voltages and currents, account for the real power flowing through the transmission line. The harmonic voltages and currents do not cause any real power flow [7].

These harmonic components can be removed, if not desired, with the use of a third harmonic trap. The inclusion of the third harmonic trap is through a transformer that is designed to provide the inductance for the trap through its magnetizing inductance [8].

The harmonic trap is included to trap the undesired third harmonic voltage, as it is the by-product of the EHM used in the model.

From equation (1.13) and (1.14), it is seen that A depends on K_0 which is the dc component of the duty cycle, while B depends on the second harmonic magnitude K_2. Therefore the line power flow given in equation (1.24) is composed of two terms – one that depends on K_0 and the other that depends on K_2 and ϕ.

Therefore, the CNT can be used to control the power flowing through a transmission line by applying the appropriate duty cycle. The CNT analysis and methodology is illustrated using a simple diagram.

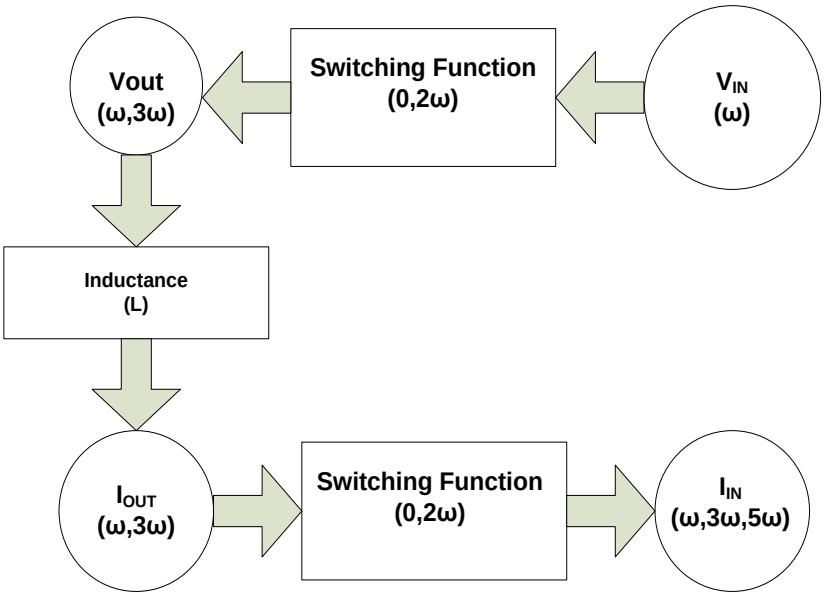

Figure 2.6: Diagram illustrating the analysis and methodology of a CNT [2].

For the purpose of proper understanding of the principle of operations of the CNT, we considered a short transmission tie-line of 100mi in length, with line inductance of 1.5mH/mi. It is assumed that the voltage angle deviation between the buses,

connected by the transmission line is 2^o. The input voltage is also assumed to be 138kV.

The amount of power flowing through the line is calculated using equation (1.24)

$$P_{line} = \frac{V_1 V_2}{\omega L} sin\delta$$

Given that,

$$\omega = 2\pi f = 376.9911 \text{ Rad/sec}$$

$L = 1.5$ mH/mile, and for a line of 100mi, L=150mH

Then,

$$P_{line} = \frac{138 \times (138) \times 10^6}{(376.9)(0.15)} \text{ sine} 2^o$$

$$= 11,756,009W$$

$$= 11.7MW$$

This is the power flowing through the line when no power flow controller is used. The power is fixed at 11.7MW.

Now, suppose a CNT with an off-nominal taps ratio of $\pm 10\%$ is place on the line. The real and reactive power flow control can be achieved by CNT, according to equation (1.24) and (1.25).

According to equation (1.24), the power flowing through the line when a CNT is connected, is given by

$$P_{LINE_{CNT}} = \frac{V_1 V_2}{\omega L}\left(A\sin\delta - \mathrm{B}\cos\left(\delta + \varphi\right)\right)$$

Where $$\mathrm{A} = \frac{1 + n - 2K_0 n}{1 - n^2}$$

$$\mathrm{B} = \frac{nK_2}{1 - n^2}$$

Using the conventional PWM, $K_2 = 0$

$$\mathrm{A} = \frac{1 + n - 2K_0 n}{1 - n^2}\ ,\ K_0 = 1[\max],\ \mathrm{n} = 0.1$$

$$= \frac{1 + 0.1 - 2(0.1)}{1 - (0.1)^2} = 0.909$$

$$\mathrm{B} = 0 \quad (\text{since } K_2 = 0)$$

Substituting for A and B in the equation (1.24), we have

$$P_{LINE_{CNT}} = \frac{V_1 V_2}{\omega L}\left(A\sin\delta\right)$$

$$= \frac{1.932\times10^{10}}{56.535}\times 0.909 sin2^{o}$$

$$= 10.8\text{MW}$$

For $K_0 = 0$ $\quad$ A = $\frac{1+n-2K_0 n}{1-n^2}$, $K_0 = 0[\text{min}]$ n = 0.1

$$= \frac{1+(0.1)}{1-(0.1)^2} \quad = 1.11$$

$$P_{LINE_{CNT}} = \frac{V_1 V_2}{\omega L}\left(A sin\delta\right)$$

$$= \frac{1.932\times10^{10}}{56.535}\times 1.11 sin2$$

$$= 13.2 \text{ MW}$$

It can therefore be seen that, using the conventional PWM techniques, the CNT can only control the real power between 13.2MW and 10.8MW. Although K_0 does not show much impact on this real power flow control, it does provide a large range of control for the reactive power [5].

However, varying K_0, the sending end reactive power can be varied from -270Mvar to 420Mvar.

The introduction of the even harmonic modulation (EHM) allows the CNT control to go beyond the range of 13.2MW and 10.8MW.This is as a result of the introduction

of the second harmonic components in the duty cycle function. EHM allows the control of the real power from -5.1MW to 28.9MW.

The control range of the power flow, with and without a CNT can be simply illustrated by the diagram below.

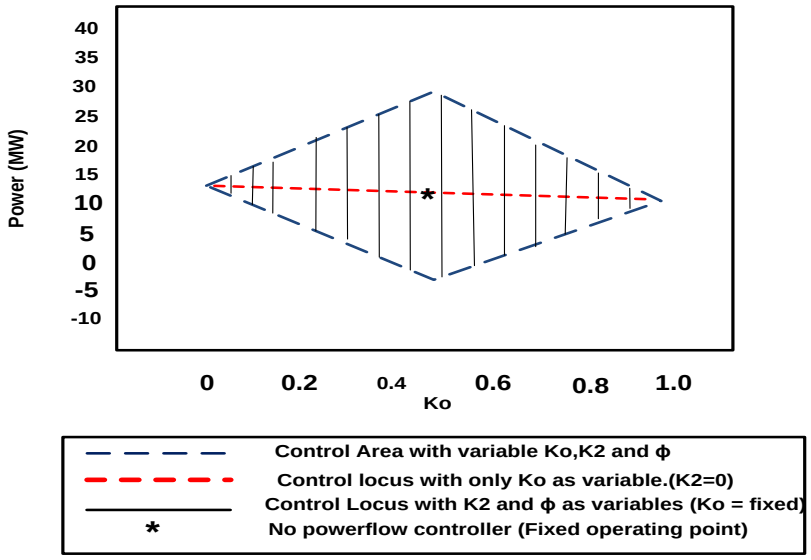

Figure 2.7: Power range control achieved using CNT [2]

It is noted that variation in K_2 does not cause much change in the real power. The overall power control area obtained by the CNT is shown in Figure 2.7 by trapezoidal area obtained in the diagram.

The variation of K_0 and K_2 affects the reactive and the real power respectively. This can be explained by the fact that K_0 affects only the output voltage magnitude while K_2 affects the angle.

Therefore, the CNT provides a wide range of control in terms of both the real and reactive power. The converters used are normally rated 20% of the transformer ratings which comes about to 5.8MVA. The areas controlled by the CNT can be

increased by increasing the value of the off-nominal tap ratio *n* [2].Increasing *n*, however, also increases the rating of the converter used.

The implementation of the converter for the CNT makes use of multilevel AC converters [2]. For example, the 5.8MVA converter for the 29MVA, a 138kV CNT is implemented by using readily available IGBT's that are rated at 1700V,1000A [2]. For a large scale transmission like this, the number of levels that will be required would be around 17-20 levels. These multilevels can be reduced by introducing step down transformers but it will introduce additional expenses [2]. Availability of new device technologies such as SiC gate turn off devices rated at 10-20 kV may make the implementation of this technology simpler at these voltage levels [2].

Chapter 3

PROJECT PROCEDURES AND SIMULATIONS

3.1 Simulink Model

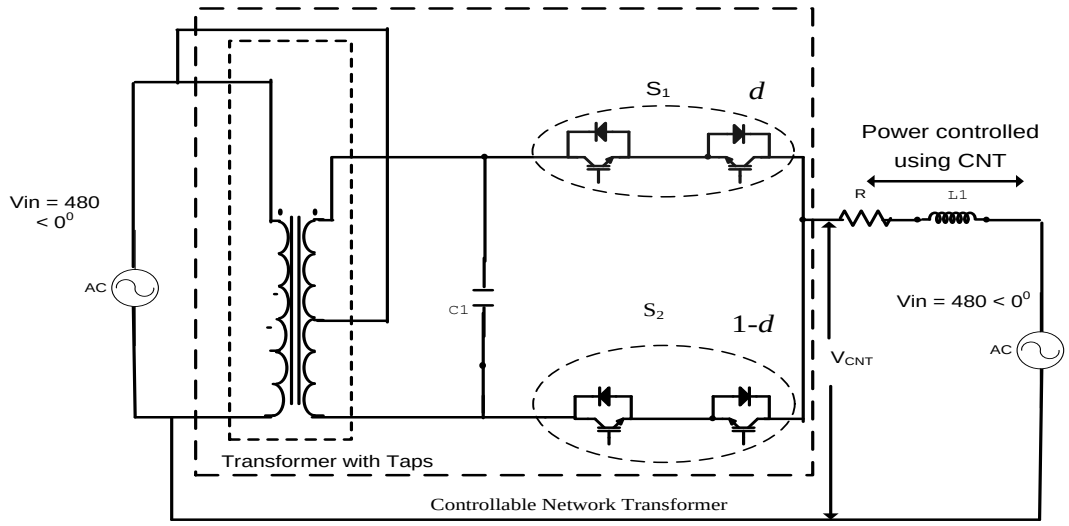

Figure 3.1: Simple circuit describing the simulation model of the CNT using MATLAB Simulink [2].

To determine, and investigate the working principles of a controllable network transformer, an experimental simulation was performed using MATLAB Simulink. The simple simulated model's topology is as seen in Figure 3.1. The topology consists of two buses (which were assumed to be at the same voltage level), line inductances, line resistances, and the controllable network transformer (CNT). The full model topology is described in the next section.

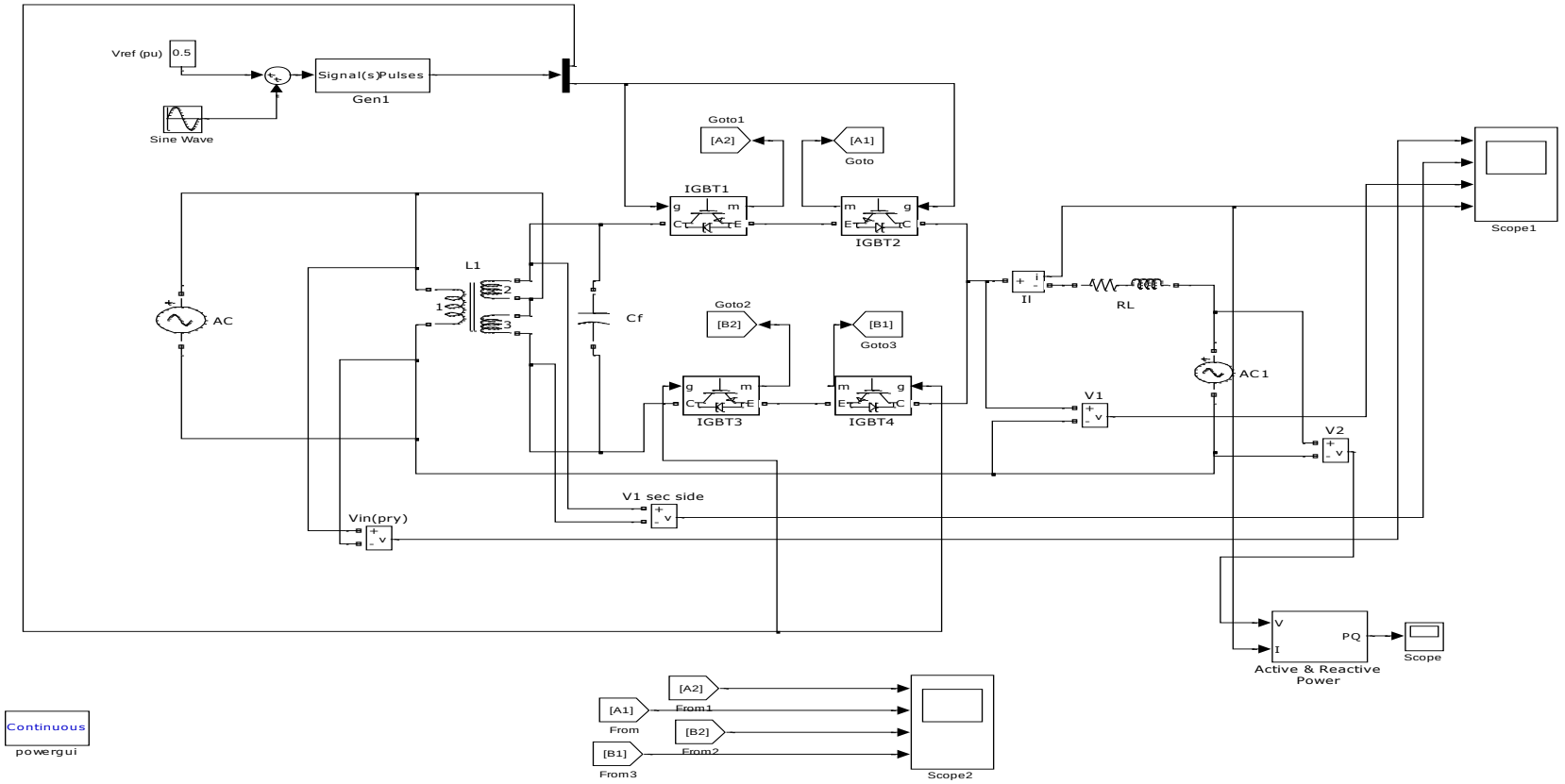

Figure 3.2: Simulation model of the CNT using Matlab Simulink

3.1.1 Brief Description of the Simulated Circuit

The simulation model as shown in Figure 3.2 consists of two voltage sources, a control source unit for the power electronics, a transformer and the RL load.

The control unit is comprised of two signal sources; which are the DC reference signal (DC component voltage) and a second harmonic source (from the sine wave). These two sources are added together and passed through a signal generator to give the desired signal pulse in driving the power electronics (IGBT's and diode's). The control unit is one of the most important components of the CNT model. It affects the overall power output ranges.

The system also consists of a two level Thin AC converter (TACC) [9] (consisting of the IGBT and an anti parallel diode). The IGBTs are usually rated 100A, 1200V and switching at 10 KHz. They are connected in such a way that they conduct in both directions. The first set of IGBT (1 and 3) conducts in the forward direction while IGBT (2 and 4) are reversed biased. Meanwhile, the current keeps flowing in the circuit as a result of the forward conduction of the diode in both directions. This is another important feature of the CNT; it allows it to be bidirectional in the control of power flow. The IGBT has an internal resistance of $1e^{-3}\Omega$, a snubber resistance of $1e^{5}\ \Omega$ and snubber capacitance made to infinite.

The input and output voltages were made to be 480V (peak). In the absence of a CNT there would be no power flow, because the two bus ends are of the same voltage. However with the CNT, the power flow magnitude and direction can be controlled.

The CNT is realized using a 480V/240 V centre-tapped transformer with an off-nominal tap ratio of 25% (that is n= 0.25) as seen in Figure 3.1. The transformer nominal power is 2KVA with a frequency of 60Hz. The transformer primary and secondary winding resistances and leakage inductances were (0.0004pu, 0.02pu) and (0.008pu, 0.046pu) respectively. These values have great impacts on the power output of the system. Hence they are fixed throughout the simulations.

It is observed that, the amount of third harmonic in the system is considerably high; therefore a third harmonic trap is added to the circuit.

The third harmonic trap is designed with a linear transformer and a capacitor. The transformer used is of a nominal power of 2kVA at frequency of 60Hz.The winding parameters are (120V, 0.008 pu, 0.046pu) for Vr.m.s, winding resistance and leakage inductance respectively. The magnetizing resistance and reactance of the transformer are kept at 20Ω and 10H respectively. The third harmonic trap is actually as a result of the capacitor (that acts as a filter) connected with the transformer. The trap capacitor's value must also be reasonable; in this analysis, its value is 3000μF. This value was picked after a series of simulations and testing in determining the best value.

A capacitor called the forward capacitor (C_f) is connected across the output of the main transformer. It functions as a filter. It filters the distortions coming from the transformer (these distortions are mostly from the leakage and magnetizing inductances of the transformer) and also those resulting from the harmonics.

The output of the CNT is looped back into its input, through a resistance and inductance of the value 3.5Ω and $10e^{-4}$H respectively.

Different oscilloscopes were connected across both the sending and the receiving ends of the model. This shows the different waveforms of the input and output voltages, voltage of the primary and secondary sides of the main circuit transformer and the current flowing. Both the active and reactive power's waveforms were also analyzed and compared with the third harmonic effects.

3.2 Experimental setup

To fully investigate the functions and working principles of the CNT, a MATLAB simulation was carried out. The simulations consist of two experimental setups:

A. Experimental setup of the CNT without a third harmonic trap
B. Experimental setup of the CNT with a third harmonic trap.

In each case, the CNT is analyzed using the main circuit topology, but the inclusion of a third-harmonic trap makes the difference. The circuit was first simulated using the conventional PWM (pulse width modulation).The use of DVQS was then considered, by injecting a second harmonic source (from the control source) to drive the power electronics. The results were computed, analyzed and reasonable conclusions reached.

The variable structure modeling of the system was also analyzed. (See section 3.4)

3.2.1 Case 1: Experimental setup of CNT without A Third harmonic Trap

The circuit topology for this procedure includes a CNT without a third harmonic trap. The trap is removed to effectively show its impact and how the harmonics affect the flow of power.

Initially, the CNT was operated using the conventional PWM techniques. Here the second harmonic amplitude, K_2 was kept at zero, while the DC component K_0 was varied from 0 to 1. This constitutes the control signal generator of the circuit and it is used in driving the power electronics (IGBT and the anti-parallel diode).

For the best results in the simulation, the value of the capacitor (C_f) used ranges between 4000µF and 5500µF. The ratings of the transformer remained the same.

The circuit was made more resistive (that is the value of the resistor used is quite larger than the reactance of the line inductance). The resistor is valued 3.5Ω while the inductive impedance was kept small ($L = 10e^{-4}H$) (it is left to be zero in an ideal circuit, but practically impossible). The input and output voltages are kept at 480V respectively.

The corresponding effects on the current and voltage waveforms were analyzed and the power outputs were also noted while K_0 was varied from 0 to 1.

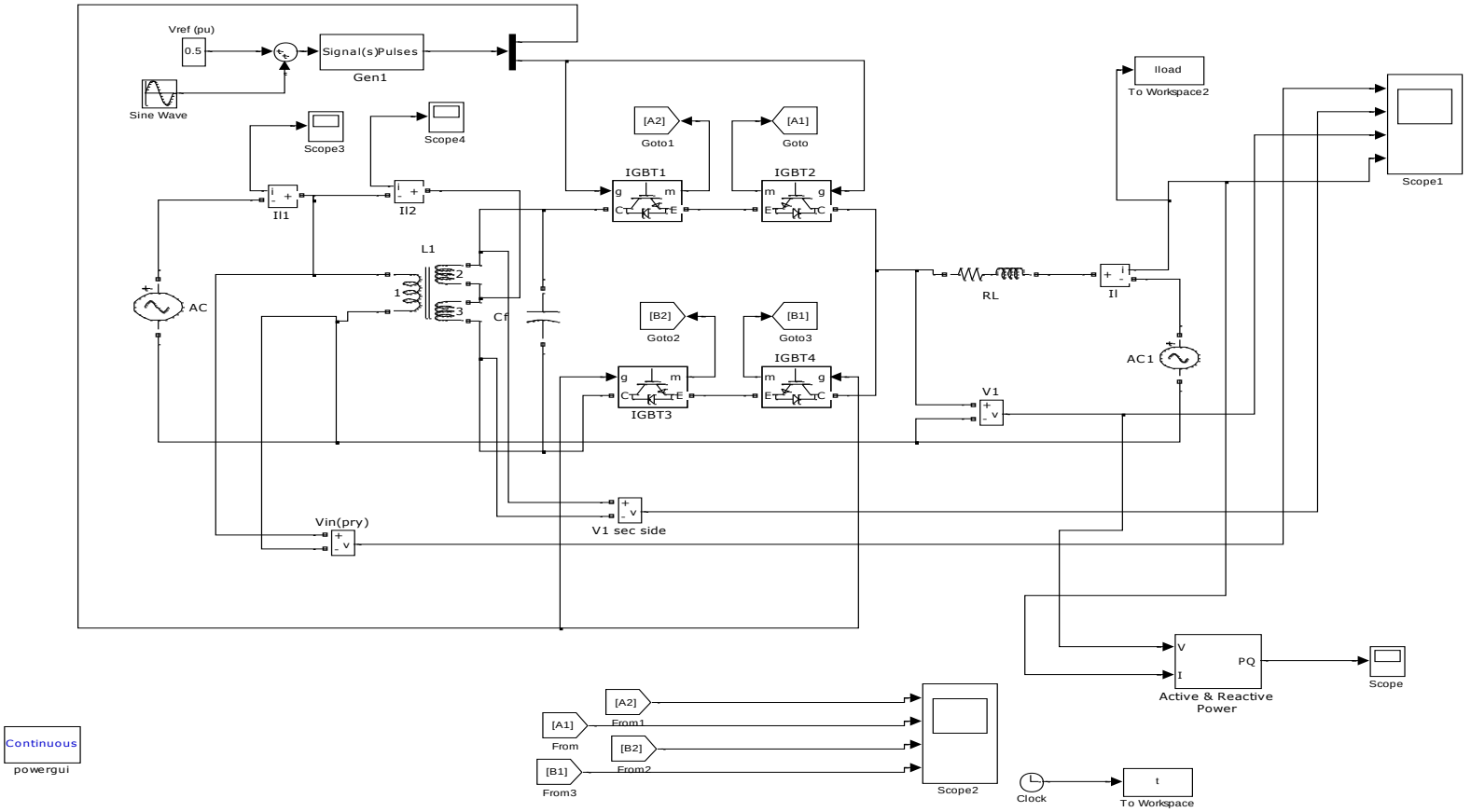

Figure 3.3: Simulation model for CNT without Third harmonic trap using MATLAB

The procedure was repeated but now K_0 and K_2 were fixed at 0.5 and 0.2 respectively (note that the summation of K_0 and K_2 must be less than or equal to 1 i.e. $K_2 \leq \min\{K_0, 1 - K_0\}$). Any combinations above this, results in over modulation.

For this second setup, the CNT was operated at two different operating points while K_0 and K_2 are kept as discussed and the phase angle (from Equation (1.1)) varied at angle 0 and 180 degrees .The circuit is made more inductive for these two operating points.

At the end of the experiment, the results were analyzed. The voltage and current waveforms for the two different experimental setups were obtained and plotted. The relationships between the output powers and K_2 (second harmonic amplitude) were also analyzed and the corresponding graphs were plotted for the two different phases (0 and 180). The effects of the capacitor's value on the output (power) were also analyzed.

3.2.2 Case 2: Experimental setup of CNT with A Third Harmonic Trap

There are no much differences in the circuit topology of the CNT with a trap and that without a trap. The main difference is the inclusion of a third harmonic trap. The trap as discussed consists of a transformer with its own parameter and configuration different from the main circuit transformer. The most important constituents of the trap are the capacitor of carefully determined values (connected across the transformer) and the value of the leakage inductance of the transformer.

The trap transformer is carefully designed to provide inductance for the trap through it magnetizing inductance. The leakage inductance of the transformer provides the functionality of the filter inductance [8].

The experimental procedure remained the same, and the input and output voltages were still 480V (peak). The forward capacitor remained 4500μF as like the one without trap. The reason for this capacitance value is to have a good comparison between the two procedures. The trap transformer is (2kVA, 60 Hz) and the winding voltage, resistance, and leakage inductances are (120V, 0.008pu, 0.046pu) respectively. The magnetizing resistance and reactance are also kept at 20pu and 10pu respectively.

The simulation was carried out by fixing K_0 and K_2 at 0.5 and 0.2 respectively while the phase angle, φ, is varied at angle 0^0 and 180^0. The output of the CNT is fed back to the input through a resistance of 2.5Ω and an inductance of $10e^{-4}$H. The model was also simulated for both 0^0 and 180^0 phase angles, by fixing other parameters and varying the capacitor C_{trap} to get the capacitance value that best traps the unwanted third harmonics in the system.

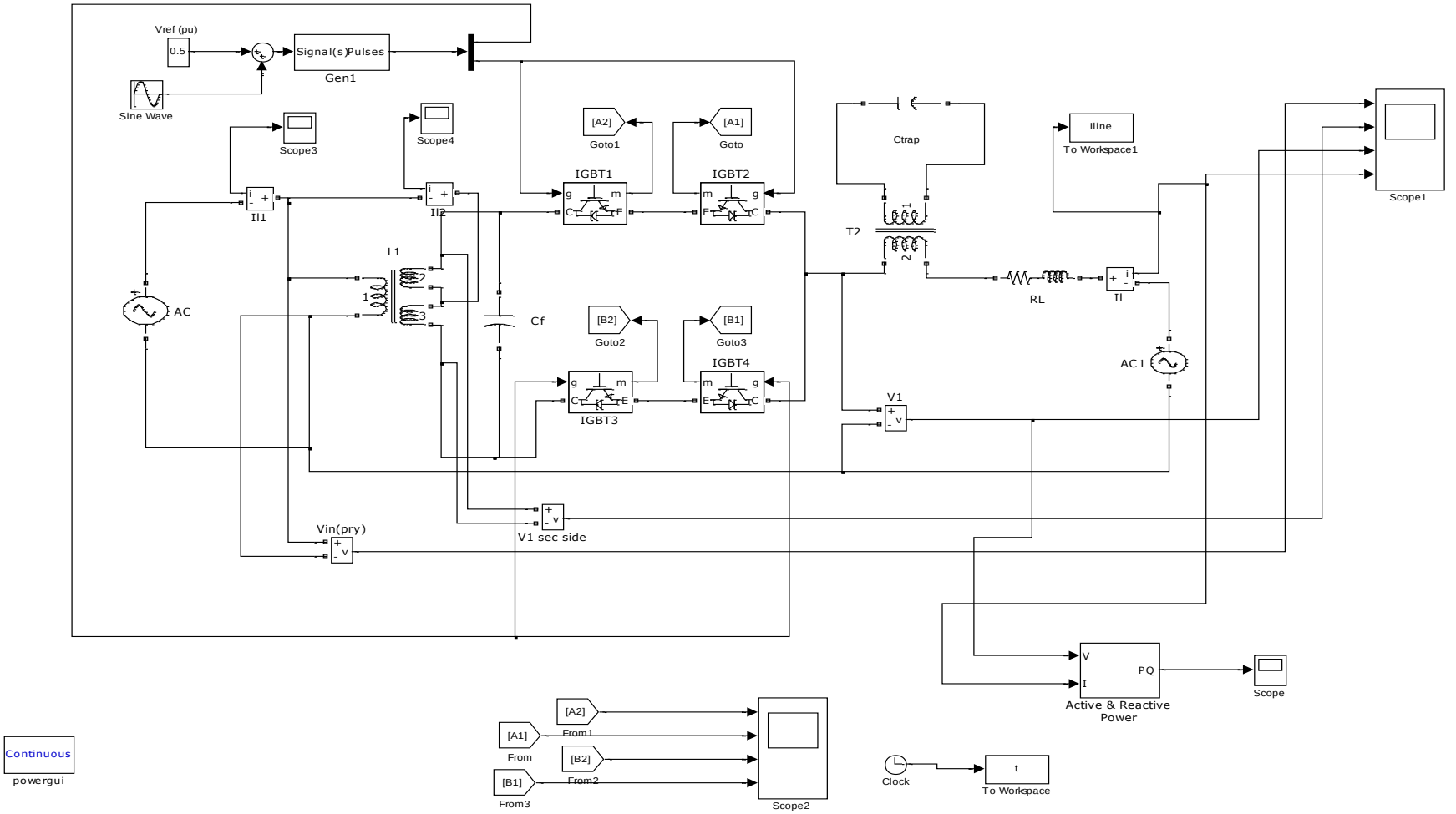

Figure 3.4: Simulation model for CNT with Third harmonic Trap Inclusion using MATLAB

3.3 Experimental results

The results obtained from the foregoing experimental procedures, are discussed in details in this section. These results are in the form of computational data, graphs and different analysis.

3.3.1 Case 1: Results and Analysis for CNT without a third Harmonic Trap

Considering the CNT analysis using the conventional PWM, the relationship between DC component amplitude (K_0) with respect to the output power (P) was investigated. It was discovered (actually confirmed) that the amplitude of the dc component cannot be more than 1. If above this value, it results in over modulation. This was shown when we checked for the value of the power at K_0 = 2.0 or 3.0. It was discovered that the power output remains the same. The output voltage from the secondary side of the transformer was full of ripples the C_f helped in reducing this ripple. The output voltage ($V_1$from Figure 3.4) of the CNT has an average voltage of 480V, but more distorted as a result of the ripples from the transformer.

The following results show the effects of change in the DC component amplitude, K_0, to the corresponding current flow in the system.

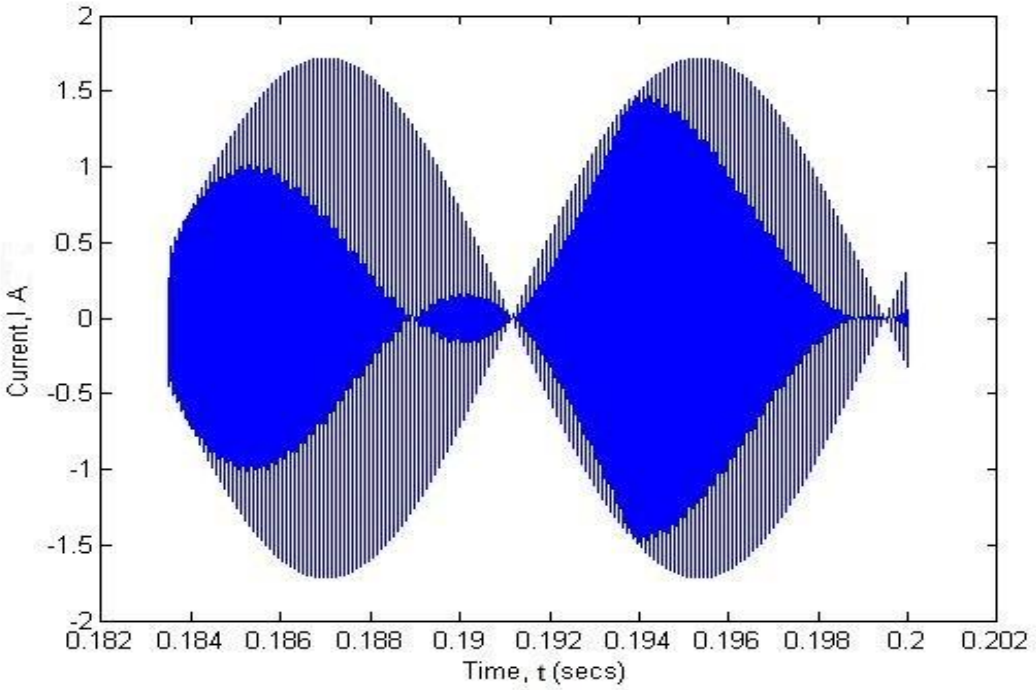

Figure 3.5: Line current when the DC component $K_0 = 0$.

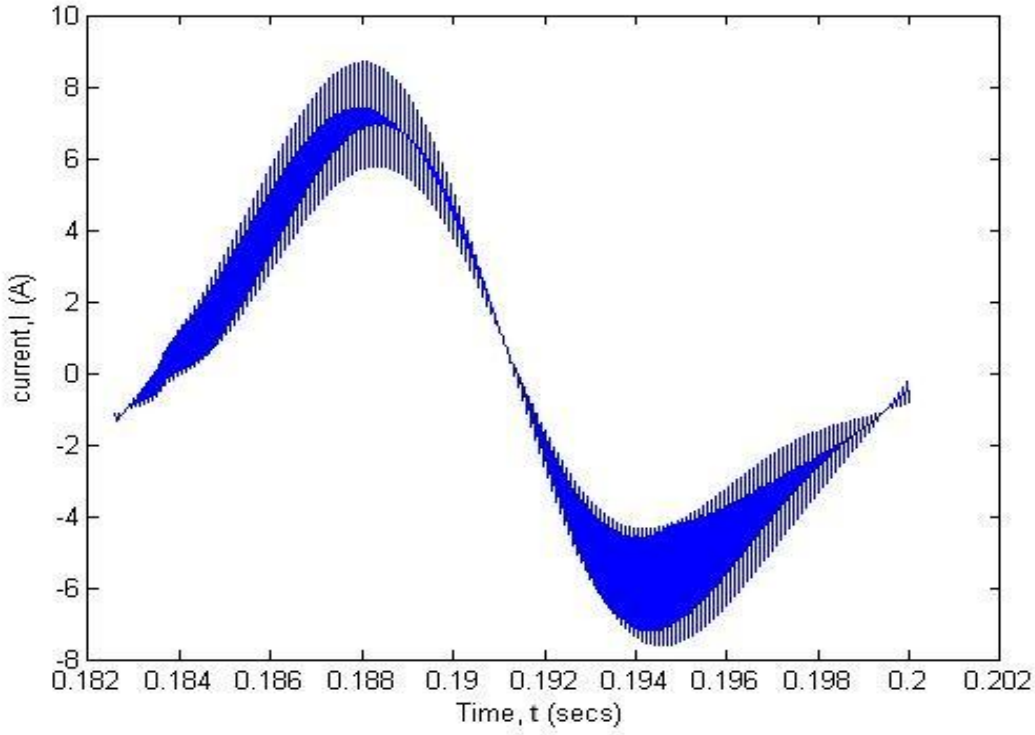

Figure 3.6: Line current when $K_0 = 0.2$

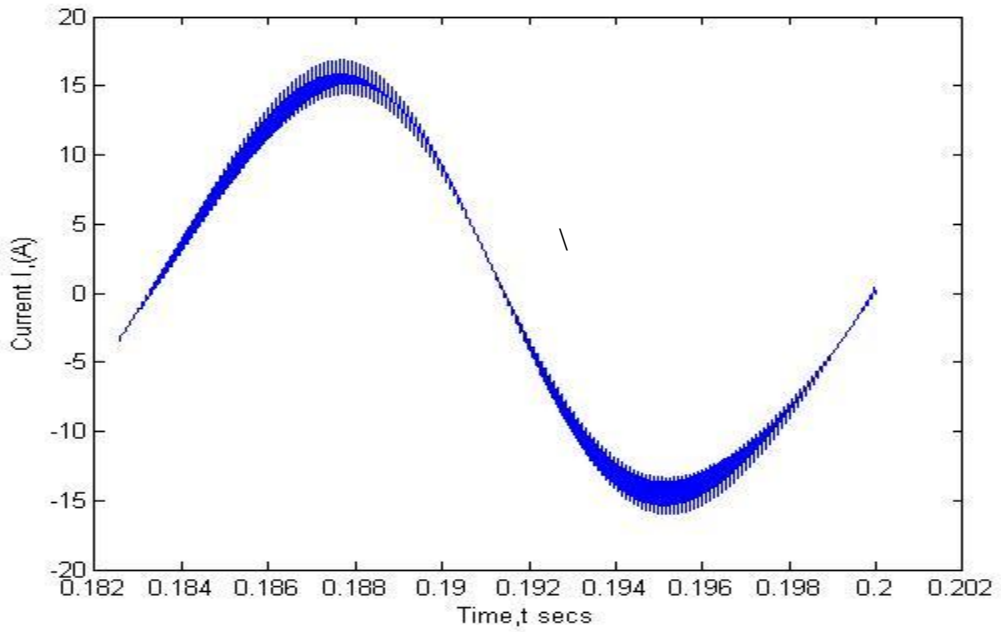

Figure 3.7: Line current when $K_0 = 0.5$

Having investigated the controlling powers of the DC component, we looked into relationship between K_0 and the power outputs.

Table 3.1: Relationship between the DC component, K_0, and the power outputs

K_0	**Power (W)**	**Q(VAR)**
0.2	1498.42	-56.55
0.4	3122.81	-123.12
0.6	4871.71	-236.41
0.8	6739.79	-415.09

These results show that there is an increase in the power outputs as the value of K_0 increases. However there is a limited range at which the power output can be varied.

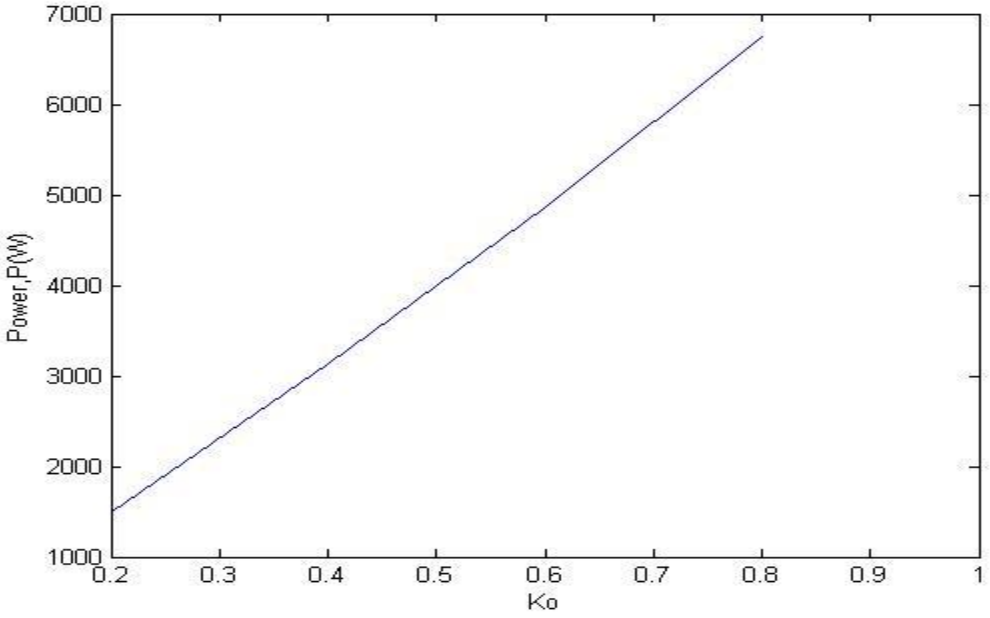

Figure 3.8: Relationship between K_0 and the Power (Watts) output

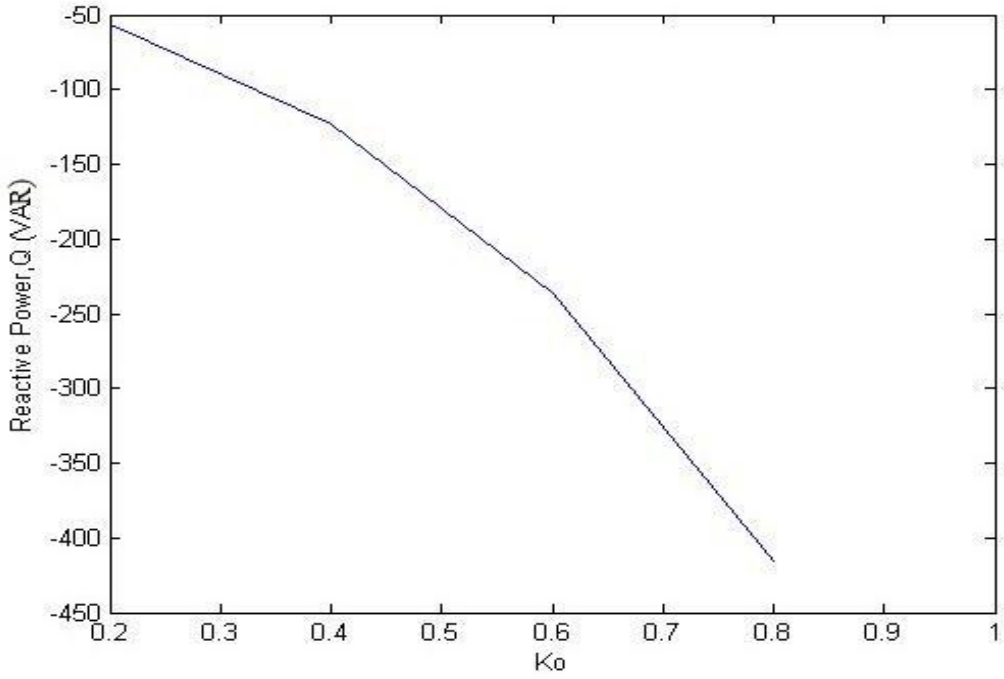

Figure 3.9: Relationship between K_0 and the reactive power Q (Vars) output

.

It is observed that the power output cannot go beyond this range. At K_0 = 0, there are little or no power flowing through the system, while at values greater than K_0 = 1.0, the system becomes unstable. Therefore, there are limitations to the amount of power flow control when the conventional PWM is used. This leads to the use of the DVQS

with EHM, where another voltage source (second harmonic) is invoked in quadrature [8] together with the DC component of the voltage to run the IGBT.

To look into the effect of this DVQS, a simple simulation was carried out. The model remained the same and third harmonic trap is not connected, the only difference is that the circuit was made more inductive.

We first considered the phase angle 0^0 while K_0 is fixed at 0.5 and the second harmonic amplitude K_2 varied between -0.4 and 0.4. The corresponding power flow with respect to the change in the K_2 is then considered. The following results were obtained.

Table 3.2: Relationship between K_2 and the power output at phase angle 0^o given $K_0=0.5$

K_2	**Power (W)**	**Q(Vars)**
-0.4	4682.70	1863.73
-0.2	5080.28	949.73
0.0	5507.69	37.31
0.2	5976.37	-869.01
0.4	6497.23	-1765.44

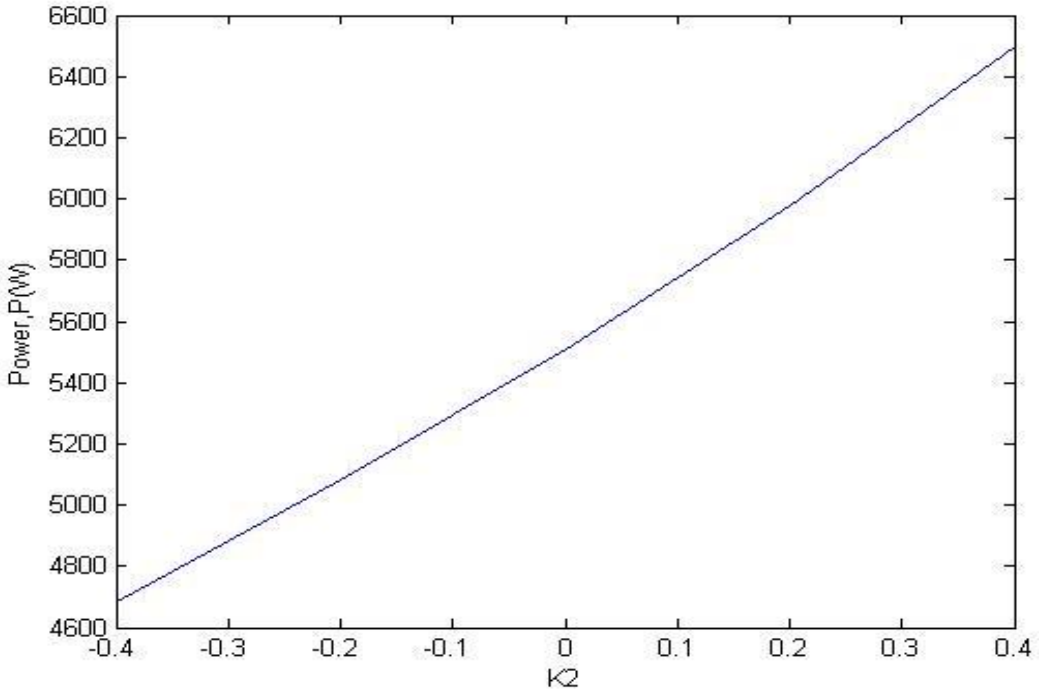

Figure 3.10: Plotting K_2 against Power (W) output at phase angle 0^0

It can be seen from the simulation results that, fixing K_0 = 0.5 and varying K_2 from -0.4 to 0.4, the CNT is able to control power from 4.6kW to 6.8kW. This conforms to what will be obtained when the equation (0.1) is used.

This thus confirmed that using the EHM (Even Harmonic Modulation) of the DVSQ, the power flowing through the CNT still falls within the range of the expected values when equation (1.24) is used.

However, the control ranges achieved by CNT allows it to have a bidirectional control of power in many situations [2]. This was further investigated by changing the phase angle to 180^0. The result is seen below.

Table 3.3: Relationship between K_2 and the power outputs at phase angle 180^o

K_2	Power (W)	Q(Vars)
-0.4	6497.23	-1765.44
-0.2	5976.37	-869.01
0.0	5507.69	37.31
0.2	5080.28	949.77
0.4	4682.7	1863.74

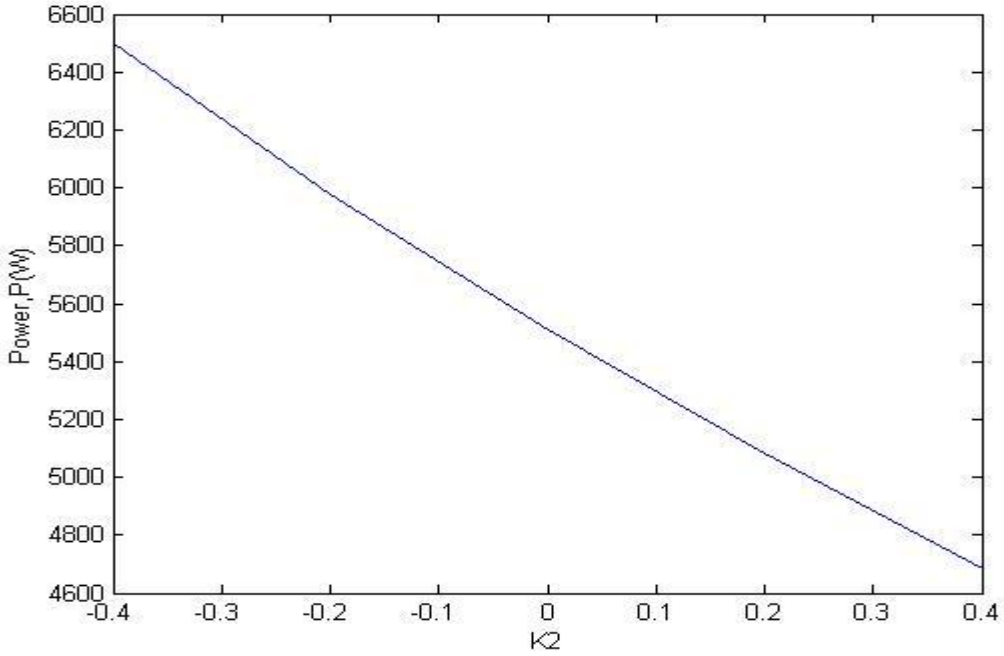

Figure 3.11: Relationships between K_2 and the Power (Watts) output at phase angle 0^0

This can also be seen in the line current waveforms. It is observed that the flow of the line current is in the opposite direction and so also is power flow, making the control by the CNT to be bidirectional.

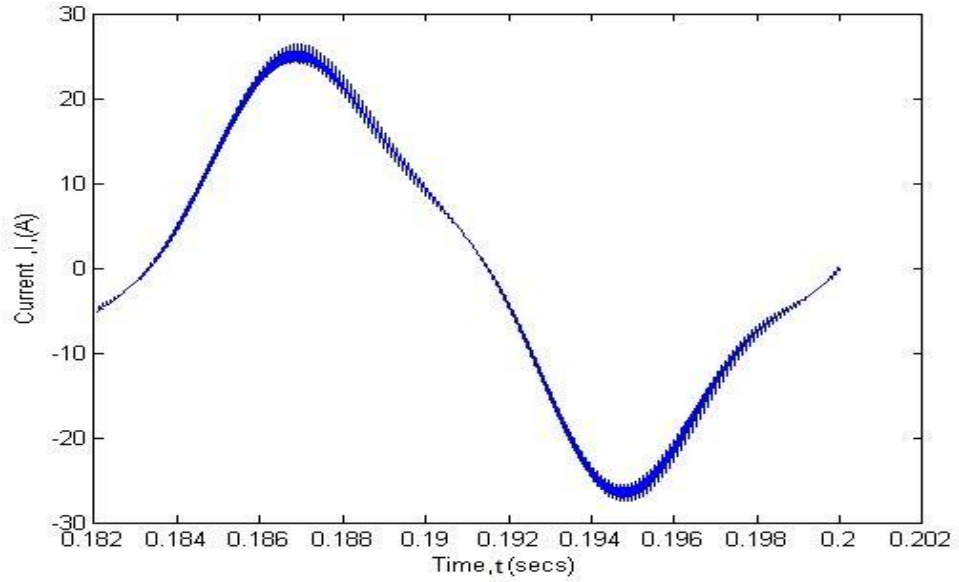

Figure 3.12: Line current waveform at a phase angle 0

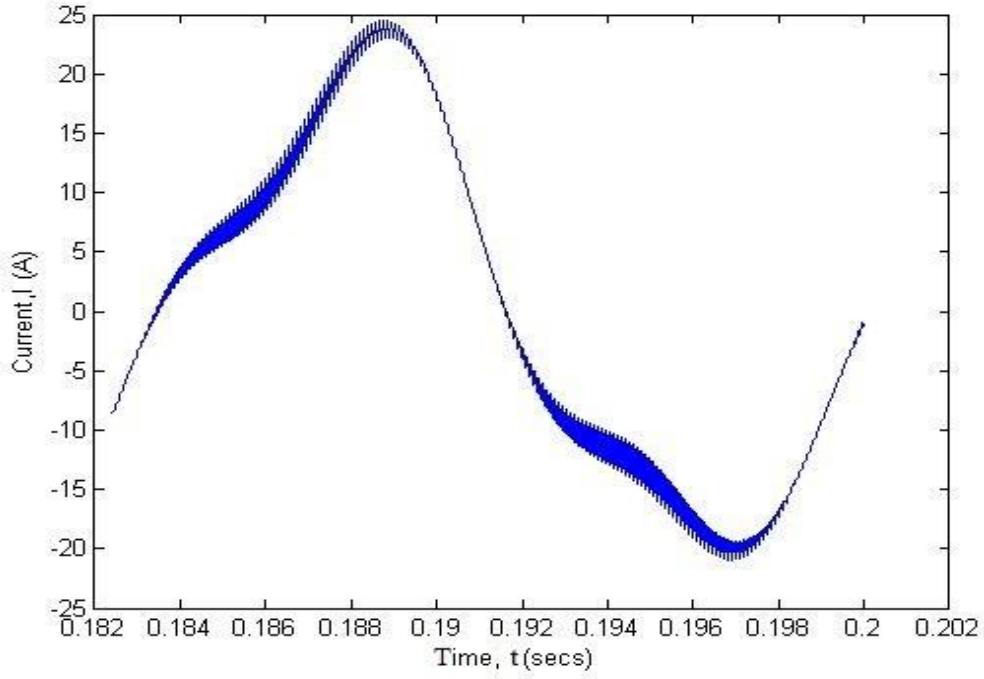

Figure 3.13: Line current waveform at a phase angle 180^0

It can be also seen that amplitude of the line current remained the same, but its direction of flow is different.

Therefore, the flow of power can be controlled by the careful adjustments of the CNT parameters (K_0, K_2 and phase angle φ). This is often very useful in the case of

contingencies (short-circuit or faults). In this case, tie line carries power from low generation areas to high generation areas thereby causing more stress on the low generation areas [2]. However, the bidirectional flow control of a CNT on tie lines prevents this kind of a situation.

Under contingencies, power flow from the area where there is fault. However, using CNT, the power in the tie line can be reversed thereby injecting the required amount of power needed to stabilize the area under contingency. Thus the bidirectional flow property of the CNT is an important property in power flow control.

However, it was noted that the amount of third harmonics in the circuit is considerably high. This is seen as evident on the amount of distortions present in the line current waveform. These harmonics need to be removed or reduced, this lead to the inclusion of a third harmonic trap to the CNT circuit.

3.3.2 Case 2: Results and Analysis for CNT with A Third harmonic Trap

The primary aim of this setup is to see the effect of the third-harmonic trap in reducing the amount of harmonics in the circuit. To be able to fully investigate this effect, the amount of the harmonics present in the circuit when the trap has not been connected was first considered.

At $K_0 = 0.5$, $K_2 = 0.2$ and phase angle $\varphi = 0^0$, the amount of the 3rd harmonics (with respect to the fundamental) in the model ,was found to be 18.4%**.**This is illustrated in Figure 3.14 below. The 3rd harmonic is seen to be considerably high.

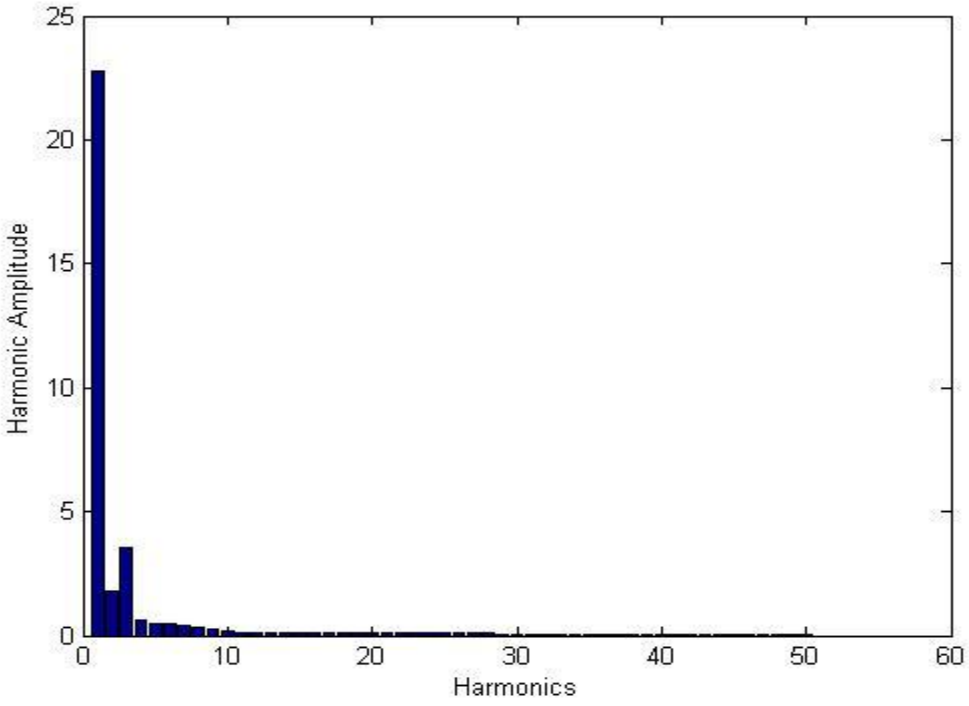

Figure 3.14: Harmonic content of the line current of the CNT model.

Table 3.4: Relationship between K_2 and the third harmonics in the CNT model without 3rd harmonic trap.

$\mathbf{K_2}$	Third Harmonic (%)
-0.4	40.2
-0.2	21.0
0	10.2
0.2	18.7
0.4	29.8

From the Table 3.4 above, the percentage of the third harmonics (with respect to the fundamental) in the model, were seen to be considerable high.

Next, the 3rd harmonic trap is connected and the value of the capacitor, C_{trap}, is adjusted to get the value that gives the lowest third harmonic in the circuit. The value of the forward Capacitor, (C_f) remained the same.

The trap capacitor (C_{trap}) is adjusted to 3000µF and the corresponding third harmonics in the circuit were examined. The following results were obtained.

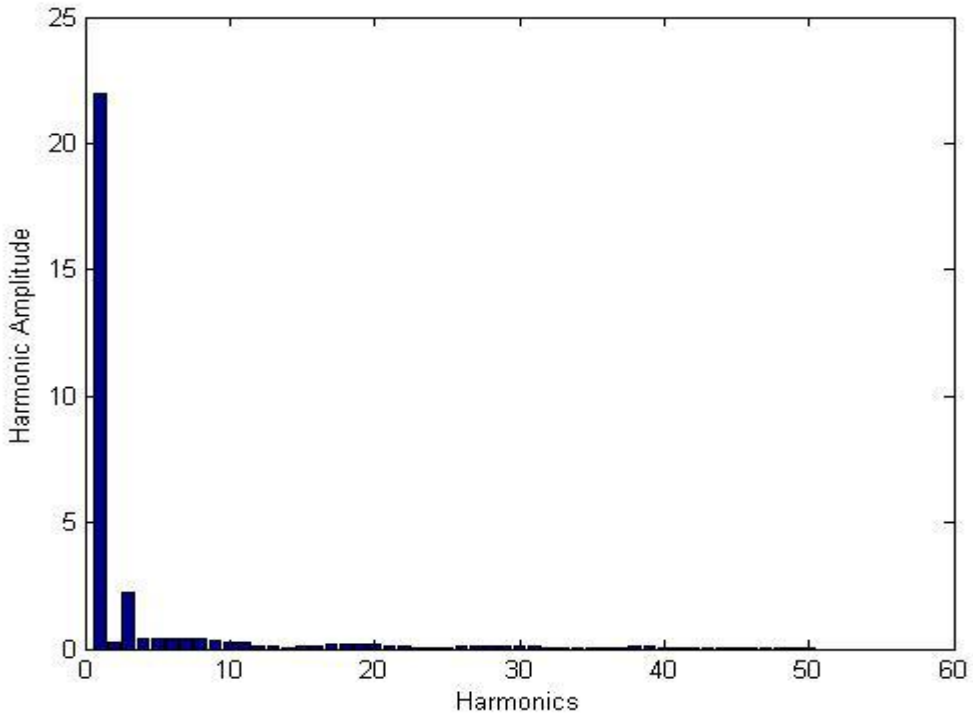

Figure 3.15: Harmonic content of the line current in the CNT circuit when 3rd harmonic trap is connected

The amount of third harmonics has been reasonably reduced to **11.45%**. Next the C_{trap} values were adjusted and the corresponding harmonic contents were measured.

Table 3.5: Relationship between C_{trap} values and the 3rd harmonics percentage with harmonic Trap connected

.

Ctrap Values (uF)	**Third harmonic (%)**
500	35.6181
1000	22.9484
1500	15.7576
2000	12.4935
2500	11.4986
3000	11.4502
3500	11.7162
4000	12.0536

The amount of third harmonic in the circuit is seen to have been reduced. The reduction, however, depends on the harmonic trap parameters. These parameters are carefully adjusted to give the optimum value of the expected power output, and at the same time to reduce or even remove the third harmonics in the circuit.

From table 3.5, the C_{trap} value that gives the lowest harmonics in the model is C_{trap} = 3000μF. Therefore, this value of the capacitor remained constant throughout the experiment. The current graph shown in Figure 3.16 shows the effect of the third harmonic trap on the line current as compared to the current waveform shown in Figure 3.12.

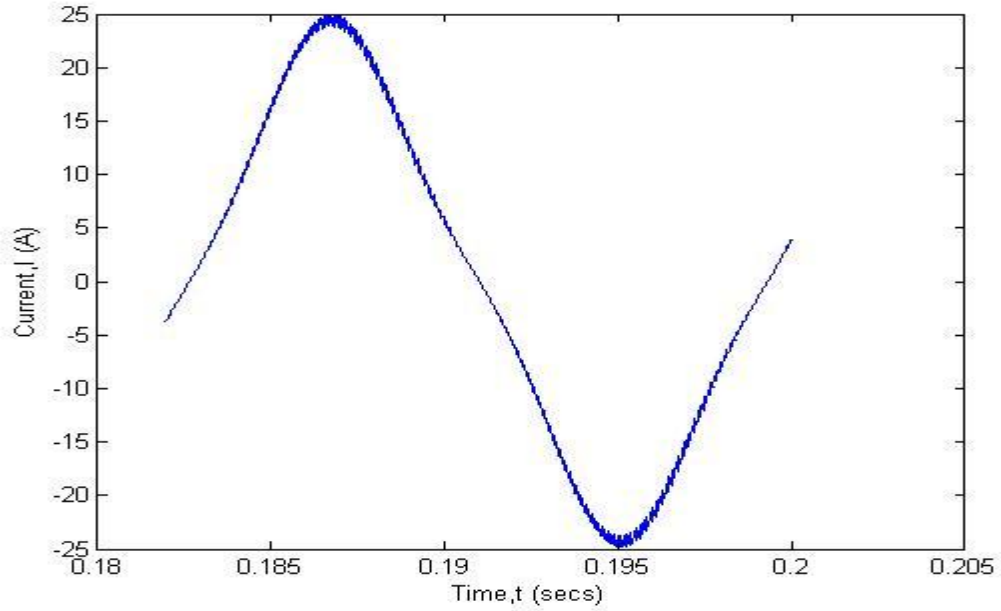

Figure 3.16: Effect of third harmonic reduction on the line current.

The current waveform is seen to become more sinusoidal. This is a result of the reduction in the third harmonic content. However, it should be noted that a third harmonic trap is not enough to trap and remove the entire third harmonics in the model. There is a need for two or more traps.

Next, we looked into the effect of the second harmonic amplitude K_2 on the third harmonics. That is, will the K_2 increase or decrease the amount of third harmonics in the system.

We considered the value of the trap capacitor that gives the minimum third harmonics in the circuit (that is Ctrap = 3000µf) while other parameters remained constant. K_2 is varied from -0.4 to 0.4 and the corresponding values of the third harmonic were measured. The results are shown in the table below.

Table 3.6: Relationship between K_2 and the corresponding 3rd harmonics with a 3rd harmonic Trap

K_2	Third Harmonics(%)
-0.4	37.4643
-0.2	23.2231
0	8.5198
0.2	11.4502
0.4	20.2078

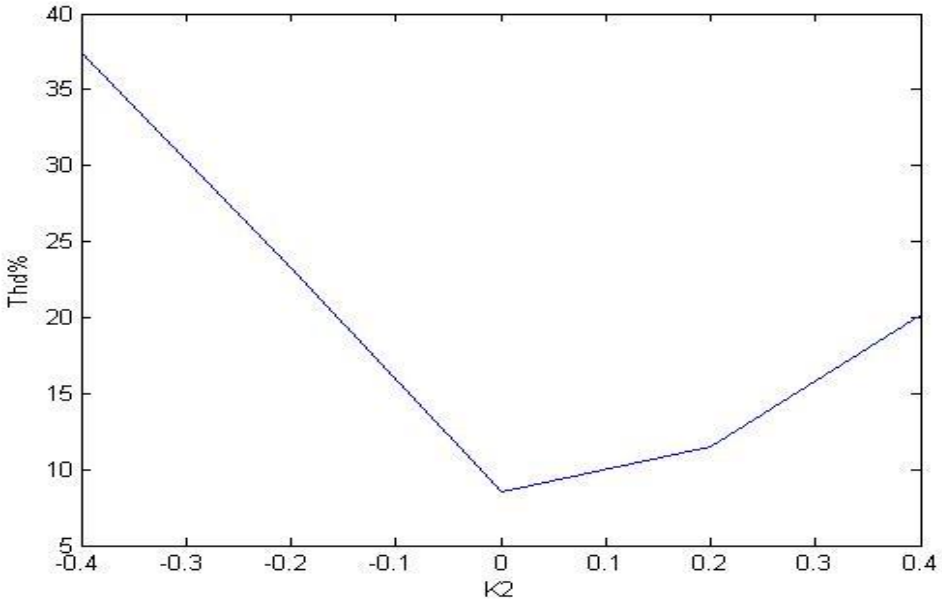

Figure 3.17: The relationships between K2 and the third harmonic contents when 3rd harmonic trap is added

It can be seen that with the proper third-harmonic trap configurations, the 3rd harmonic contents of the line current could be removed or reduced to its minimum values.

3.4 CNT Variable Structure System Model

The analysis of the variable structure system of the CNT model from Figure 3.1 is been considered in this section. This enabled us to obtain a model that explains the principle of working of the CNT in a more comprehensive way. It also allowed us to predict the behavior of the system according to the function *d* (duty cycle). The VSS model also allowed us to know how to redesign the system using the control model.

To analyze the variable structure system of the controllable network transformer (CNT), the circuit in Figure 3.18 is considered.

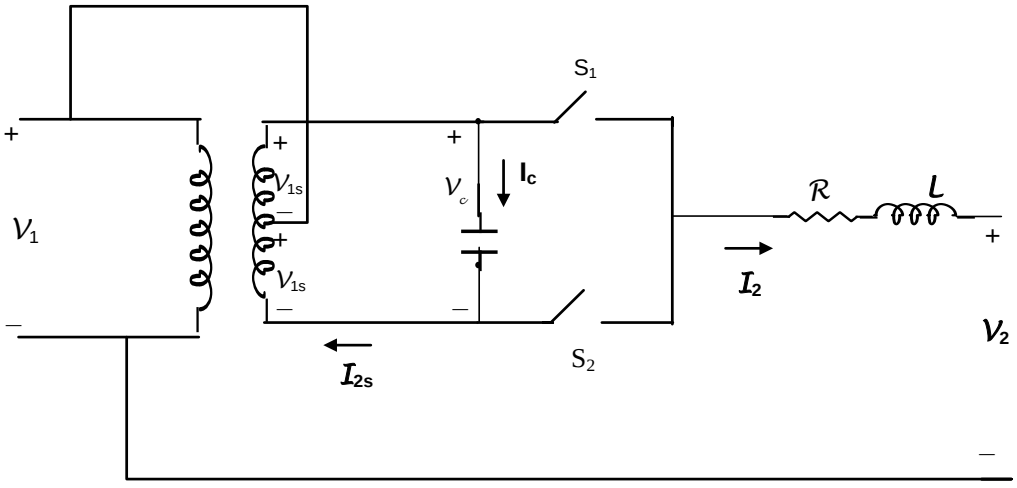

Figure 3.18: The CNT Model showing variable structure system.

The variable structure system model's equations are derived as follows;

For the Voltage across the circuit, using KVL

When duty cycle $d = 1$ (S_1 Closed)

$$L\frac{di_2}{dt} + Ri_2 + V_2 = V_1 + V_{1s} - L_l\frac{di_{1s}}{dt} \tag{3.1}$$

Also at duty cycle, $d = 0$ (S_2 Closed)

$$L\frac{di_2}{dt} + Ri_2 + V_2 = V_1 - V_{1s} - L_l\frac{di_{1s}}{dt} \tag{3.2}$$

Combining Equation (3.1) and (3.2), we get

$$L\frac{di_2}{dt} + Ri_2 + V_2 = V_1 - (2d-1)V_{1s} + L_l[-d\frac{di_{1s}}{dt} + (1-d)\frac{di_{1s}}{dt} \tag{3.3}$$

For the capacitor's current,

When $d = 1$

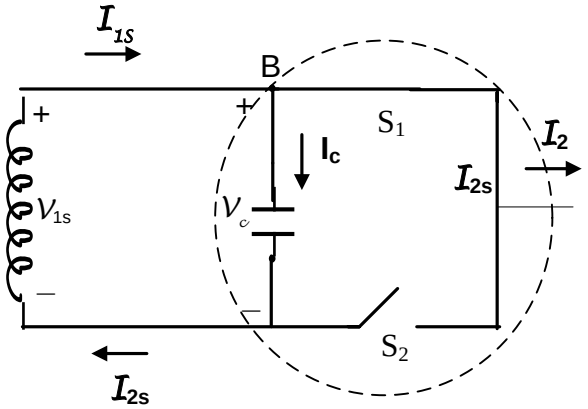

Figure 3.19: Flow of current when S1 is closed

Taking KCL in the loop, we have

$$i_c = i_{1s} - i_2 \tag{3.4}$$

Also

At $d = 0$

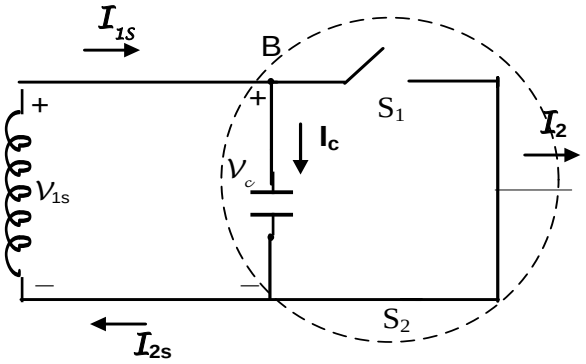

Figure 3.20: Flow of current when S2 is closed

Taking KCL at node B from Figure 3.20

$$i_c = i_{1s} - i_2 \tag{3.5}$$

Combining equations (3.4) and (3.5)

$$i_c = (1-d)i_{1s} + di_{2s} \tag{3.6}$$

The KCL for the super node becomes

$$i_{1s} - i_{2s} - i_2 = 0$$

$$i_2 = i_{1s} - i_{2s} \tag{3.7}$$

KVL for the loop (V_{1s},V_{2s},V_c)

$$V_c = 2V_{1s} - L_l \frac{d}{dt}(i_{is} + i_{2s}) \tag{3.8}$$

Using Equation (3.7), the term in the square brackets in equation (3.3)

$$-d\frac{di_{1s}}{dt}+(1-d)\frac{di_{2s}}{dt}$$

$$=-d(\frac{di_2}{dt}+\frac{di_{2s}}{dt})+(1-d)\frac{di_{2s}}{dt}$$

$$=(1-2d)\frac{di_{2s}}{dt}-d\frac{di_2}{dt}$$

Therefore equation (3.3) becomes

$$[L+L_l d]\frac{di_2}{dt}+Ri_2+V_2=V_1+(2d-1)V_{1s}+L_l[1-2d]\frac{di_{1s}}{dt} \quad (3.9)$$

From equation (3.6) and (3.8)

$$C\frac{dV_c}{dt}=i_c=(1-d)(i_2+i_{2s})+di_{2s} \quad (3.10)$$

Also, from equation (3.7) and (3.8)

$$V_c=2V_{1s}-L_l\frac{d}{dt}(i_{is}+2i_{2s}) \quad (3.11)$$

Multiplying equation (3.11) by *d* and rearranging

$$L_l d\frac{d}{dt}(i_2+2i_{2s})=d(2V_{1s}-V_c) \quad (3.12)$$

Also, rearranging equation (3.9)

$$L\frac{di_2}{dt} + L_l[d\frac{di_2}{dt} + 2d\frac{di_{2s}}{dt}] - L_l\frac{di_{2s}}{dt} + Ri_2 + V_2 = V_1 + (2d-1)V_{1s} \quad (3.13)$$

Substitute (3.12) in (3.13)

$$L\frac{di_2}{dt} + d(2V_{1s} - V_c) - L_l\frac{di_{2s}}{dt} + Ri_2 + V_2 = V_1 + (2d-1)V_{1s} \quad (3.14)$$

From Equation (3.11)

$$2L_l\frac{di_{2s}}{dt} + L_l\frac{di_2}{dt} = 2V_{1s} - V_c \quad (3.15)$$

Multiplying (3.14) by 2 and adding it to (3.15)

$$(2L + L_l)\frac{di_2}{dt} + 2d(2V_{1s} - V_c) + 2Ri_2 + 2V_2 = 2V_1 + 2(2d-1)V_{1s} + 2V_{1s} - V_c \quad (3.16)$$

$$(2L + L_e)\frac{di_2}{dt} = (2d-1)V_c - 2Ri_2 + 2(V_1 - V_2) \quad (3.17)$$

From equation (3.15)

$$2L_l\frac{di_{2s}}{dt} = 2V_{1s} - V_c - L_l\frac{di_2}{dt} \quad (3.18)$$

Substituting $\frac{di_2}{dt}$ from equation (3.17) into (3.18), this becomes

$$2L_l\frac{di_{2s}}{dt} = 2V_{1s} - V_c - L_l[-\frac{2R}{2L + L_l}i_2 + \frac{2d-1}{2L + L_l}V_c] + \frac{2(V_1 - V_2)}{2L + L_l} \quad (3.19)$$

Let

$$L_e = L + \frac{1}{2}L_l$$

Where *Le* = Total impedance
L= Line Impedance
L_l = Magnetizing Impedance

Therefore, from equation (3.10, 3.17 and 3.19), we have

$$\frac{di_{2s}}{dt} = \frac{1}{L_l}V_{1s} - \frac{1}{2L_l}[1 + \frac{L_l}{L_e}\left(d - \frac{1}{2}\right)]V_c + \frac{R}{2L_e}i_2 - \frac{(V_1 - V_2)}{2L_e} \tag{3.20}$$

$$\frac{di_2}{dt} = -\frac{R}{L_e}i_2 + \frac{1}{L_e}(d - \frac{1}{2})V_c + \frac{(V_1 - V_2)}{L_e} \tag{3.21}$$

$$\frac{dV_c}{dt} = \frac{1}{C}(1-d)i_2 + \frac{1}{C}i_{2s} \tag{3.22}$$

Equation (3.20), (3.21) and (3.22) are the major equations that make up the control system of the circuit.

Considering $d = \frac{1}{2}$ and $v_1 = v_2$

$$\frac{di_{2s}}{dt} = -\frac{R_l}{L_l}i_{2s} - \frac{1}{2L_l}V_c + \frac{R_T}{2L_T}i_2 + \frac{1}{L_l}V_{1s} \tag{3.23}$$

$$\frac{di_2}{dt} = -\frac{R_T}{L_T}i_2 \tag{3.24}$$

$$\frac{dV_c}{dt} = \frac{1}{C}i_2 + \frac{1}{C}i_{2s} \tag{3.25}$$

Meanwhile, at a steady state; $i_2 \to 0$

$$\frac{di_{2s}}{dt} = -\frac{R_l}{L_l} i_{2s} - \frac{2V_{1s} - V_c}{2L_l} \tag{3.26}$$

$$\frac{dV_c}{dt} = \frac{1}{C} i_{2s} \tag{3.27}$$

With equations 3.20, 3.21 and 3.22, the control or the variable structure system of the CNT is easily analyzed.

These equations represent the CNT in terms of the switching function *d.* It helps in the prediction of the behavior of the system, in terms of the duty cycle *d.*

The VSS may also help in the design of the system as well as analyzing it. It should be noted, however, that it becomes more complicated as it is time-variant and cannot be analytically solved easily.

Using the above derived equations, we investigated the principles of working of the CNT and the level of third harmonics expected in the circuit, when a third harmonic trap is not included in the system. It also allowed us to determine the amount of traps needed to fully remove the 3rd harmonics in the system.

The line current waveform obtained, are also compared with the ones obtained in the main CNT circuit.

The effects of the leakage resistance, the leakage inductance, the line resistance and line inductance, on the system were also considered.

3.4.1 Brief Descriptions of the CNT Control Model

The model was developed from the equations obtained from the variable structure system of the CNT model. As seen in Figure 3.21, the CNT model comprises of the duty cycle generator (which consists of the DC component, K_0 and a second harmonic amplitude K_2 and the phase angle φ), different gains and oscilloscopes for measurements.

The line resistance and inductance were 2.5Ω and $10e^{-4}$H respectively. The main transformer leakage resistance (R_l) and leakage inductance (L_l) were also made 0.1152Ω and $6.5e^{-4}$H respectively (these values were carefully picked after a series of experiments using different values). The value of the capacitor remained 4500μF. Both the sending and the receiving end voltages were assumed to be the same (480V) and the CNT has an off-nominal tap ratio of 25%.

As seen in from the derived equations, the transformer resistances and inductances were accounted for. However, it is to be noted that the IGBT and diode resistances were not put into considerations. This is due to the complexity in the derivation of the equations, which takes into account the IGBT and the diode resistance for the model. The control circuit of the CNT for this simulation is shown in Figure 3.21

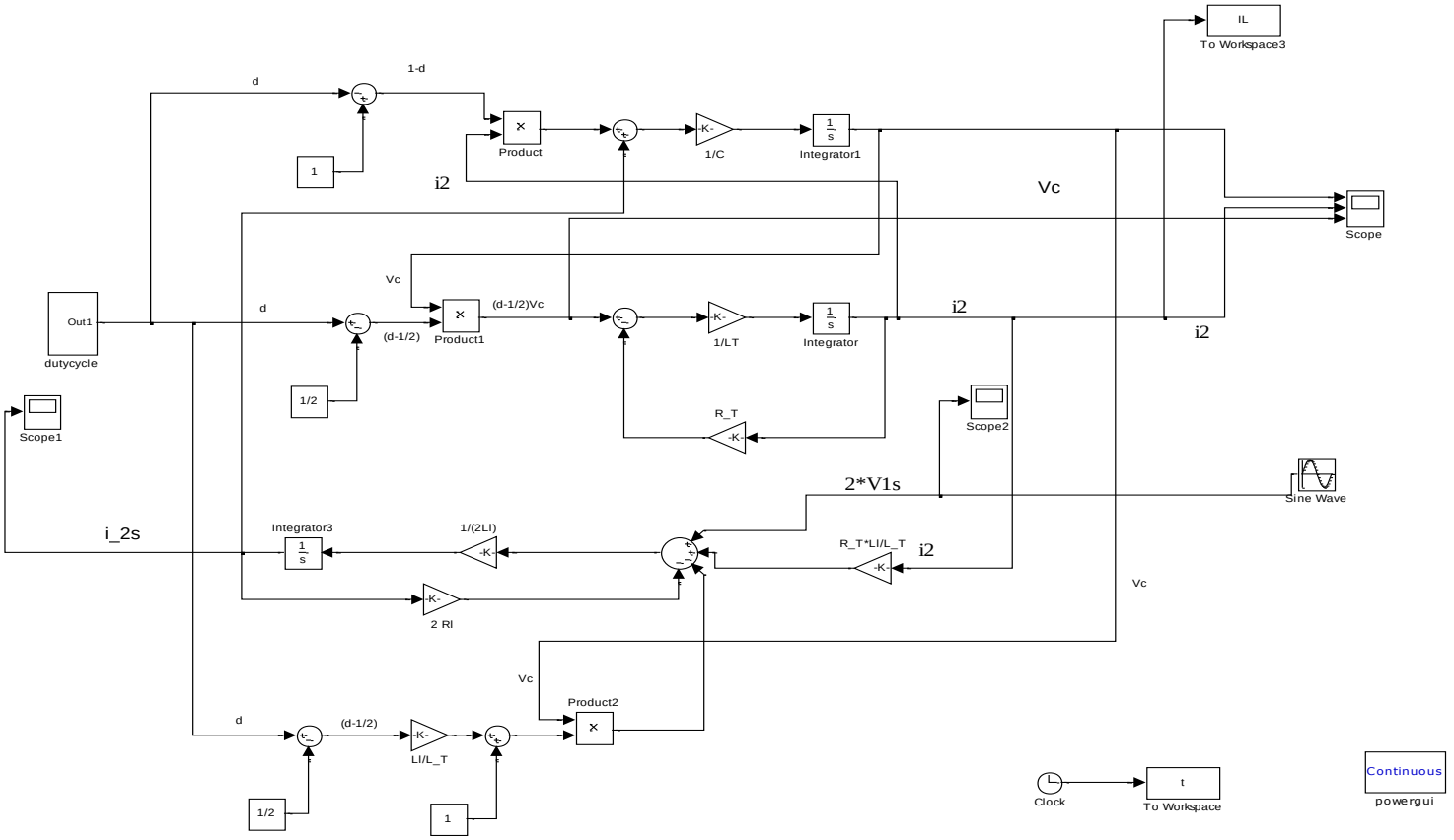

Figure 3.21: Control model of the CNT circuit.

3.5 Experimental Procedure

The procedure was carried out using the MATLAB simulink. The simulated model is the same as the model shown in Figure 3.21.

The simulation was carried out by fixing K_0 and K_2 at 0.5 and 0.2 respectively while the phase angles, φ are varied (at angle 0^0 and 180^0).The circuit is made more inductive.

3.5.1 Results and Analysis for the Control CNT.

From the simulations, we were able to get the actual behavior of the CNT. The actual current waveform is given below.

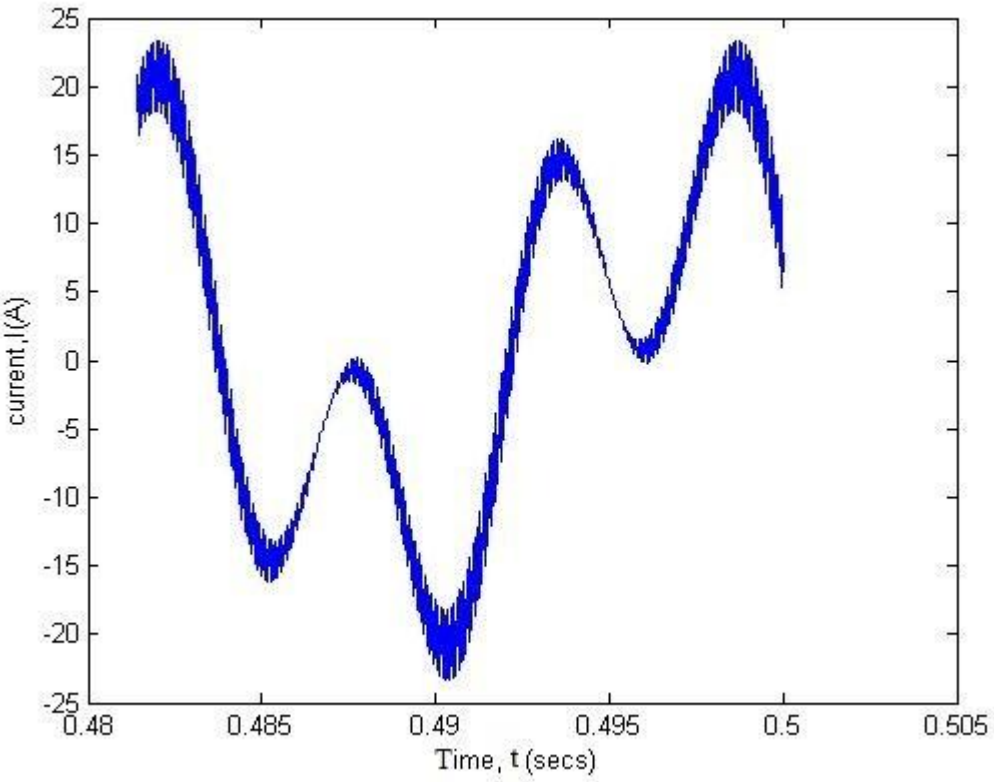

Figure 3.22: Line current waveform at a phase angle 0^0

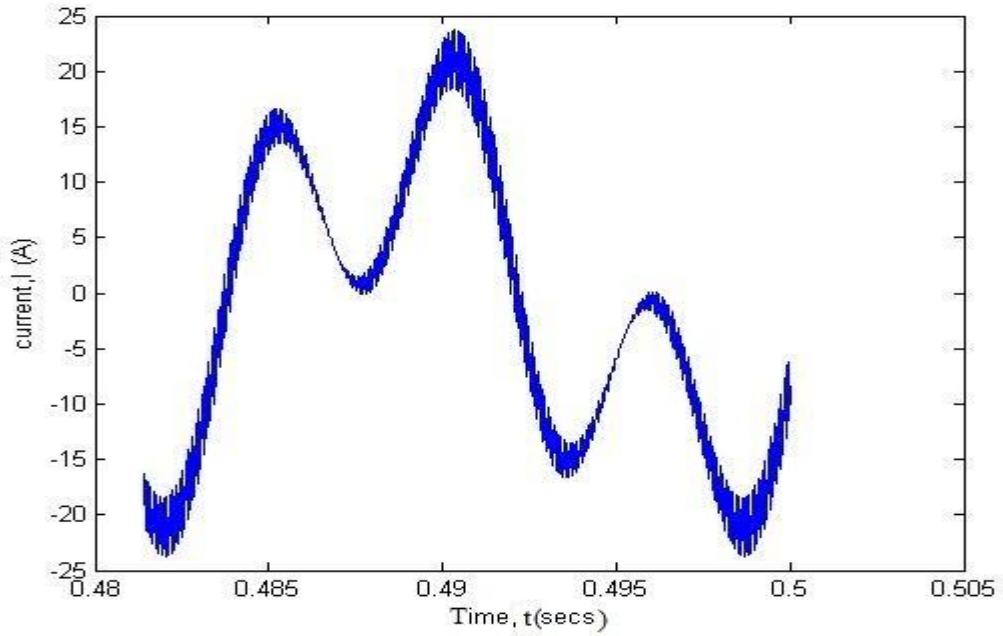

Figure 3.23: Line current waveform at a phase angle 180^0.

It is observed that the current flows in the opposite direction when the angle was change to 180 degrees. The third harmonic is seen to be high in the current waveform.

Another important observation is that the flow of power in the circuit depends highly on the leakage inductance and leakage resistance of the main transformer. Reducing the resistances shoot up the current flowing through the line. Also, increasing the leakage inductance distorts the current waveform while reducing the current in the circuit.

Setting K_0 = 0.5 and K_2 = 0, there are no current flowing through the circuit. Therefore the control effort of the CNT, in the form of second harmonic, is at its peak at this point.

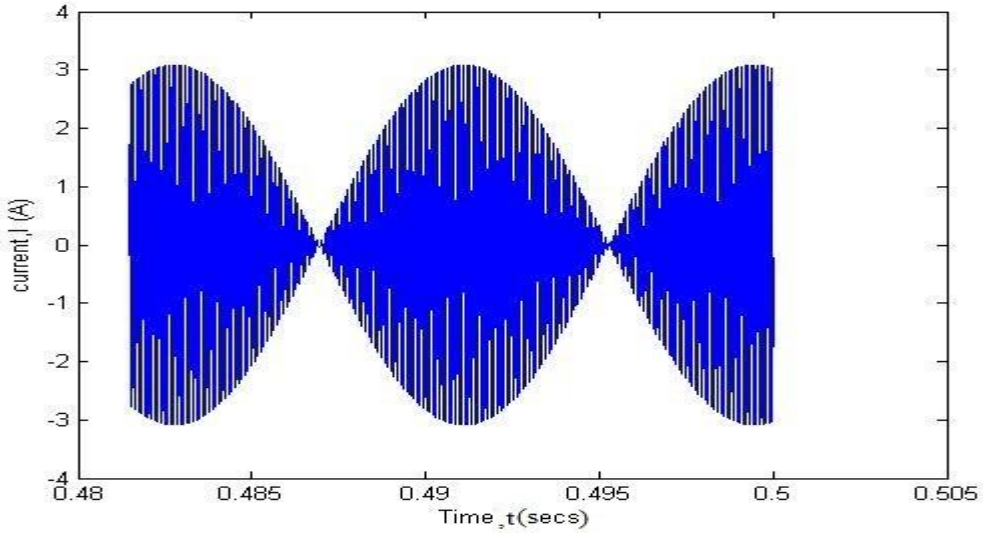

Figure 3.24: Current in the control circuit at $K_0 = 0.5$ and $K_2 = 0$.

It is also observed that the harmonic injection was at its peak here. This is shown in the diagram below.

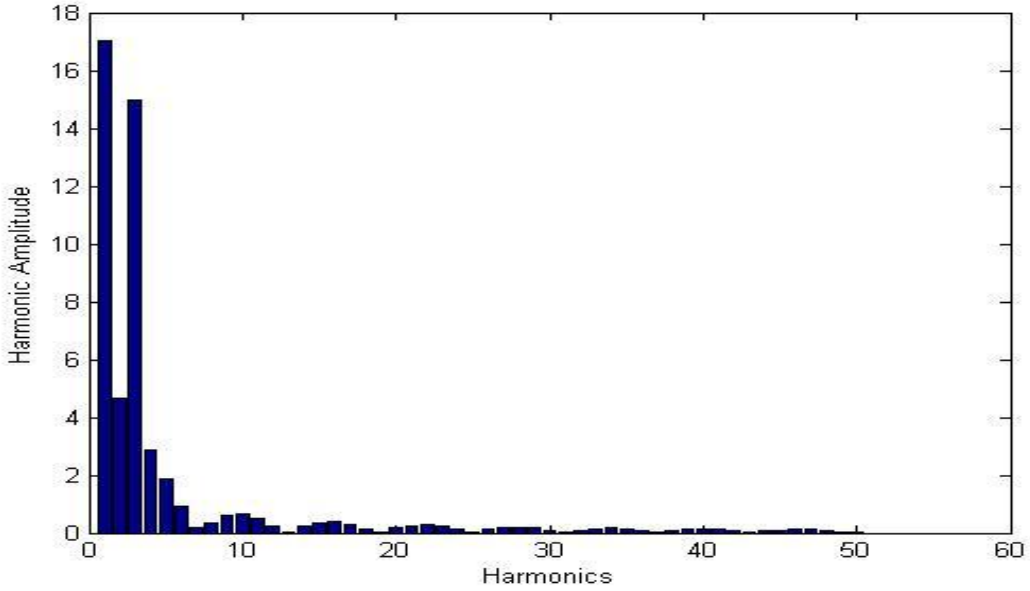

Figure 3.25: Harmonic content of the control circuit at $K_0 = 0.5$ and $K_2 = 0$.

The amount of third harmonics in the circuit with respect to the fundamental is as high as 94.96%. This shows the necessity for one or more third-harmonic trap in the use of CNT to control power flow in a system. However, in some utilities, power flow can be controlled to a reasonable level by limiting the amount of harmonic injected in the circuit [4].

From the control analysis of the CNT, we are able to predict its principle of working. Comparing the current waveforms obtained from the variable-structure model and those obtained from the experimental set-up given in section 3.2, shows that the variable-structure model is more successful in describing the behavior of the CNT. The reason for this may be the mismatch in the parameters of the actual system in section 3.2 and those of the power electronics model. In any case, the variable-structure model has been shown to be a reliable tool for representing the behavior of the CNT. Hence, it can be used to analyze and design such a system.

3.6 Discussions

From the simulations, we were able to find out that the CNT is independent of the phases to control the flow of power. This is an edge the CNT has over the other power flow controllers. In the case of a BTB, all the phases are connected to one or a common DC link, while in the PST there is an interconnection between all the phases involved [2]. The implication of this is that, a fault on one of the phases is reflected to the others [2].

Since most faults are single phase, this interaction between the phases causes the disturbances to increase. Therefore it would be more challenging in setting protective relays on these power controllers [2]. This is avoided in the CNT.

Secondly, the CNT requires only one transformer that handles just only a portion of the rated power. This is unlikely in the case of BTB and the VTF that requires two transformers respectively to step down the line voltage. These transformers are required to carry a fully rated power.VTF are basically rotating transformers that handle the entire power [2]. For implementation purposes, 8-10 VTF’s are often

required and operated in parallel in order to share load [2]. The CNT uses an existing transformer and therefore reduces the cost of installation significantly.

In the case of the BTB, the converters are required to handle the full rated power. The CNT converters only need a portion of the power as compared to the transformer ratings. In the case of this thesis, only 25% of the transformer ratings were used.

Like the BTB and the VTF, the CNT can vary the power flow in both directions. This is seen in Figure2.7 and experimentally in Figure 3.20 and Figure 3.21 by changing the phase angle of the duty cycle generator. The full bidirectional capability of the CNT is achieved by controlling all the parameters simultaneously (that is K_0, K_2, and φ). The bidirectional capability of the CNT reverses the flow of power, and injects the needed power into the system in the case of contingencies. The BTB and VTF are known to have wide controllability as compared to CNT, because they can have full control over the power flowing through the line [2].As seen from simulations, the control range of the CNT is quite high but might not be as wide as the BTB and the VTF since it is covering just a portion of the system [2].

The loss of one or more devices in the CNT will not have much impact on the operation of the systems [2], unlike in the case of BTB and the VTF, where there would be negative impacts on the network operations with meaningful margin.

Therefore in a mesh network with multiple CNT, the operators are expected to have more meaningful and flexible controllability than a network with just one or more central point power flow controllers.

On the last note, the CNT has a ‘Fail Normal” operation mode [7]. This occurs when there is a converter failure. The CNT can convert and restore itself to a normal transformer by bypassing the semiconductor switches. This is seen in Figure 3.9 when the K_0 is varied and K_2 kept at 0. This is very important in the case of a failure of a converter, the line reliability is restored back to it normal state [2].

Chapter 4

CONCLUSION, CRITICISM AND FUTURE WORK

4.1 CONCLUSIONS

In this thesis, we carried out a series of simulations on the Controllable Network Transformer in controlling the flow of power between two power system areas.

In the first set of simulations, we checked the effects of the control signals of the CNT (DC component, the second harmonic and the phase angle) on the general working of the CNT. It was observed that these three components of the control source have great influence on the controllability property of the CNT. With proper adjustments of the DC component, second harmonic component and the phase angle, the CNT is made to control power flow in a system as desired.

Secondly, a series of simulations were carried out to test the effect of the leakage inductance and resistances of the main transformer, the forward capacitance, line inductance and resistances and the effect of the third harmonic on the overall system

Thirdly, the variable structure model of the system was developed to analyze the working principle of the CNT. We were also able to see the effect of the duty cycle *d* on the overall working of the CNT.

In conclusion, the CNT has a great potential in its ability to control the power flow through a wide range, when compared to other power flow controllers. It also has a

way of trapping the unwanted third harmonic through a well designed third harmonic trap used in the system.

Finally, the MATLAB simulation results proved the operating principles of the CNT regarding wide controllability of the power flow in a tie line between two areas.

4.2 CRITICISM OF THE CNT APPROACH

The principle of working of the CNT has been extensively discussed in this thesis. The CNT approach seems applicable and if properly implemented, it will go a long way in controlling the flow of power in the ever challenged smart grids.

However, in the course of this thesis, the numerous simulations carried out in MATLAB Simulink on the CNT has allowed us to make the following critics of the proposed (from [7]) power flow controller.

Firstly, it has been shown that there is a large third harmonics in the line current. This is an unwanted situation. A third harmonic trap, as discussed in the thesis, will not be enough to remove all the unwanted harmonics. There will be a need for more traps at the higher transmission level and this makes the CNT more complicated and expensive to build.

Secondly, the CNT has been discussed at a small scaled transmission level. However, for higher power transmissions, there are needs for switches with high power ratings. There will also be a need for the IGBT to be connected both in series and parallel connection. Therefore, the model becomes more complicated at this high level transmission.

Finally, the amount of the injected reactive power is considerably high. The amount of these reactive powers in the circuit, need to be regulated. Too much of reactive powers in a transmission line, increase the apparent power resulting in low power factor. To increase the power factor, however, a reactive power compensator should be added.

4.3 FUTURE WORK

In the future, it is recommended that the CNT be made to work together with other power flow controllers. The Static Synchronous Compensator (STATCOM) is recommended. This is because the STATCOM is an active filter that works mainly as a compensator. The switching control strategy of the STATCOM is to switch the devices rapidly on and off. This will result in a pulse modulated line voltage with variable magnitude and phase presented by a large fundamental component and a handful of high frequency harmonics [17]. The resulting high frequency harmonics in the model can be removed or filtered, using high frequency tuned passive elements of the STATCOM [17].

The STATCOM connected with the CNT can work in two ways; when the source voltage is larger than the fundamental voltage of the converter, the STATCOM generates reactive power, and when system voltage is higher, it absorbs reactive power [17].

Therefore, the STATCOM allows the device to absorb or generate controllable reactive powers with an apparent capacitive or inductive current absorbed by the controlling bridge and it is independent of the AC line voltage level with respect to the converter voltage [17].

REFERENCES

[1] Min D., Mohammad N.M et al, "Power Flow Control of a Single Distributed Generation Unit with Non Linear Local Load*", Power Systems Conference and Exposition, PES. IEEE,* pp 398-403 vol.1. 10-13 Oct. 2004.

[2] Das D., Divan D., *"*Power Flow Control in Networks Using Controllable Network Transformer*" IEEE Transaction on Power Electronics,* pp 1753 - 1760, July 2010.

[3] James D.W., "*Implementation of Newton-Based Optimal Power Flow into A Power System Environment"*, Thesis: University of Illinois, Urbana-Champaign, Illinois, 1997.

[4] Rusnak J. "*Power Flow Control by the use of Phase shifting Transformer"*, PhD Thesis, FEI TU, Kosice, 2003.

[5] Rusejla S. "*Power Flow Control With UPFC"*, Internal Report, Zurich, 2004.

[6] Einar L, Richard P., et al, "Variable Frequency Transformer- a New Alternative for Asynchronous Power Transfer", *GE Energy and Hydro-Quebec TransEnergie,* 2004.

[7] Divan D., Sastry J. "Controllable Network Transformers" *Power Electronics Specialist Conference, PESC. IEEE,* pp 2340- 2345, 15-19 June 2008.

[8] Das D., Divan D., Sastry J., "Voltage Synthesis Using Dual Virtual Quadrature Sources- A New Concept in AC Power Conversion". *IEEE Transactions on Power Electronics*, pp 3004-3013, vol. 23, issue: 6. Nov 2008.

[9] Das, D., Divan D, et al., "Thin AC Converter –A New Approach for Making existing Grid assets Smart and Controllable", *Power Electronics Specialist Conference, PESC, IEEE*, pp 1695-1701, 15-19 June 2008.

[10] Dommel H.W, Tinney W.F., "Optimal Power Flow solutions", *IEEE Transaction On Power Apparatus and Systems*, pp 1866-1876, vol. PAS-87, Issue 10. Oct 1968.

[11] Wood A.J., Wollenberg B.F., "*Power Generation operation and Control"*, New York. John Wiley & Sons, Inc., Page 39,517. 1996.

[12] Sun D.I., Ashley B. et al, "Optimal Power Flow By Newton Approach", *IEEE Transaction on Power Apparatus and Systems*. pp 2864 -2880.Vol. PAS-103, Issue: 10. Oct 1984.

[13] Alsac O., Bright J., et al., "Further Development in LP- based Optimal Power Flow", *IEEE Transaction on Power Systems*, pp 697-711, Vol. 5.Issue 3. August 1990.

[14] Yu-Chi W., Debs A.S. et al., *"*A Direct Nonlinear Predictor –corrector primal-dual Interior point Algorithm for Optimal Power Flows*", IEEE Transaction on Power Systems*, pp 876-883, Vol. 9, Issue 2, May 1994.

[15] Hingorani, N.G., *Gyugyi L.,* "*Understanding Facts: Concepts and Technology of the Flexible AC Transmission Systems",* New York, IEEE Press, 2000.

[16] Bagen B., Jacobson D., et al., "Evaluation of the Performance of Back to Back HVDC Converter and Variable Frequency Transformer for Power Flow in a weak Inter connection", *Power Engineering Society General Meeting. IEEE,* pp 1-6, 24-28 June 2007.

[17] Strzelecki R., Benysek G. "*Power Electronics in Smart Electrical Energy Networks*" London, Springer-Verlag London limited, 2008.

[18] Raczkowski B.C., Sauer P.W., "*Modeling, Simulation and Analysis of Variable Frequency Transformer*", Thesis: University of Illinois, Urbana-Champaign, Illinois, 2006.

[19] Transformer on Load Tap Changer (2011, June). Retrieved November 2011, from Transmission lines design and Electrical Engineering hub http://www.transmission-line.net/2011/06/transformers-on-load-tap-changer.html

[20] Quadracture booster (2011, July 1). Retrieved November 2011, from Wikipedia http://en.wikipedia.org/wiki/Quadrature_booster